

Improving the selectivity of the  
radio-labelling of ion exchange resin tracers  
for positron emission particle tracking



Michael van Heerden

Dissertation presented for the degree of Master of Chemical Engineering  
in the Department of Engineering  
University of Cape Town

July 2015

The copyright of this thesis vests in the author. No quotation from it or information derived from it is to be published without full acknowledgement of the source. The thesis is to be used for private study or non-commercial research purposes only.

Published by the University of Cape Town (UCT) in terms of the non-exclusive license granted to UCT by the author.

**DECLARATION**

I, the undersigned, know the meaning of plagiarism and declare that all the work in the document, save for that which is properly acknowledged, is my own.

Signature: .....

M. R. van Heerden

Date: .....

# Abstract

Positron emission particle tracking (PEPT) is a technique which non-invasively tracks tracer particles labelled with a positron emitting radionuclide in a system of flow. The tracers are tracked through the detection in a PET scanner, of the two nearly collinear 511 keV gamma rays resulting from the annihilations of the positrons. For this technique to be effective, the tracer must be representative of the media in the system under study, and labelled with a sufficient activity of radionuclides. Organic ion exchange resins are suitable tracer materials for PEPT experiments, and are usually labelled with  $^{68}\text{Ga}$  at the laboratories of PEPT Cape Town. The labelling performance relies on the chemical and physical properties of organic strongly acidic cation exchange resins and the nuclear chemistry of  $^{68}\text{Ga}$ . The objective of this study is to obtain consistent tracer labelling throughout, or even beyond, the lifespan of the  $\text{SnO}_2$   $^{68}\text{Ge}/^{68}\text{Ga}$  generator which degrades over time.

The objective is achieved by integrating a purification technique into a “standard” radiolabelling method used at iThemba LABS. A small 0.5 ml Amberchrom CG-71 column is loaded with the  $^{68}\text{Ga}$  generator eluent in 7 M HCl, then rinsed of most the contaminants before eluting the product with distilled water and used in the radiolabelling method. Using a 1-year-old 30 mCi  $\text{SnO}_2$   $^{68}\text{Ge}/^{68}\text{Ga}$  generator eluent that has been purified by this method improved the radiolabelling performance by an average of at least 10% when compared to the performance of the un-purified product.

Purifying the generator eluent will enable PEPT experiments of longer duration, and in highly shielded systems where tracers with high activity are required, such as granular and fluid flow in engineering applications.

# Acknowledgements

There are several people who I am indebted to who have made the last two and half years possible. Firstly, my supervisor Professor J-P Franzidis who took me on as a student and gave me the opportunity to develop myself and never hesitated to make sure I had all the resources I needed. My co-supervisor and mentor Professor Andy Buffler, who inspired me to keep improving and showed unwavering patience through it all.

Huge thanks go to Katie Cole, for the dedication, guidance, continued support and countless hours of discussion, friendship and the time I needed for anything and everything.

And to my dearest Sarah, your kind heart and relentless dedication in keeping my spirits high will not be forgotten. Thank you for the days of carrying my burdens and bringing joy to my life when I needed it most.

Thank you to my colleagues at RPD, especially to Selwyn De Windt and Sebastian Losper for helping me with your expertise, strong interest and positive attitudes towards research. Thanks and gratitude should also go to Stuart Dolley, for always engaging me with your mountain of knowledge. To my previous supervisor, Nick, for patiently teaching me things that I only came to understand a bit later in life.

To my family, for making me the person I am today. This work is the result of your encouragement, love and life lessons bestowed upon me. And to my friends, who always kept me sane and feeling human.

To my colleagues and friends in Physics, who gave me their time, support and kind words; thank you for the gift of working with you.

Last but not least, the South African Research Chairs Initiative of the Department of Science and Technology and National Research Foundation of South Africa (NRF) for funding this research through the Minerals to Metals research initiative.



# Table of Contents

<b>Chapter 1</b> .....	1
Introduction.....	1
1.1 Research objectives, questions and scope .....	4
<b>1.1.1 Objectives</b> .....	4
<b>1.1.2 Hypotheses</b> .....	4
<b>1.1.3 Scope</b> .....	5
<b>1.1.4 Key questions</b> .....	5
1.2 Organisation of thesis .....	6
<b>Chapter 2</b> .....	7
Radionuclides for PEPT.....	7
2.1 Positron decay.....	7
2.2 Positron emission particle tracking.....	8
2.3 Production of tracers for PEPT.....	12
<b>2.3.1 Tracers produced by the direct activation method</b> .....	12
<b>2.3.2 Tracers produced by chemical sorption methods</b> .....	13
<b>2.3.3 Tracers produced by the “drill and fill” method</b> .....	15
2.4 Properties of ion exchange resins .....	16
<b>2.4.1 Exchange capacity</b> .....	17
<b>2.4.2 Equilibrium measurements for ion exchange resins</b> .....	17
<b>2.4.3 Interactions of ion exchange materials</b> .....	19
<b>2.4.4 Resins used at PEPT Cape Town</b> .....	20
2.5 <sup>68</sup> Ga for ion exchange in PEPT.....	22
<b>2.5.1 SnO<sub>2</sub> <sup>68</sup>Ge/<sup>68</sup>Ga generators</b> .....	23
<b>2.5.2 Contaminants in an SnO<sub>2</sub> <sup>68</sup>Ge/<sup>68</sup>Ga generator</b> .....	24
<b>2.5.3 Methods to purify the <sup>68</sup>Ga eluate</b> .....	27
<b>Chapter 3</b> .....	31
Experiments.....	31
3.1 Reagents and equipment.....	31
3.2 Resin and column preparation .....	33
3.3 Equilibrium distribution coefficients.....	35

3.4	Separation method .....	36
3.4.1	Elution profiles.....	36
3.4.2	Column separation .....	37
3.4.3	Method to determine column size .....	38
3.5	Tracer labelling comparison test.....	38
<b>Chapter 4</b>	.....	<b>39</b>
Results and Discussion	.....	39
4.1	Equilibrium distribution coefficients, $K_d$ .....	40
4.2	Separation method .....	43
4.2.1	Elution profiles.....	43
4.2.2	Modified separation method .....	49
4.2.3	Column separation .....	51
4.2.4	Separation method improvements .....	56
4.3	Modified separation method performance.....	58
4.4	Tracer labelling comparison test.....	60
4.5	Summary.....	62
<b>Chapter 5</b>	.....	<b>65</b>
Conclusion	.....	65
5.1	Limitations of the work .....	66
5.2.1	Purification of $^{68}\text{Ga}$ .....	67
5.2.2	System enhancements.....	67
<b>References</b>	.....	<b>69</b>

# List of Figures

Figure 2.1: Illustration of the decay path of a positron emitted via $\beta^+$ decay.....	8
Figure 2.2: The gamma rays detected by the PET scanner. ....	10
Figure 2.3: ECAD “EXACT3D HR++” PET scanner located at PEPT Cape Town. ....	11
Figure 2.4: Overview of the standard radiolabelling procedure.....	15
Figure 2.5: Two examples of the "drill and fill" method.....	16
Figure 2.6: Illustration of a cationic exchange resin .....	17
Figure 2.7: $\text{SnO}_2$ $^{68}\text{Ge}/^{68}\text{Ga}$ generator (left), iThemba LABS generator (right).....	23
Figure 2.8: Separation factors of various ions relative to $\text{Ga}^{3+}$ (from literature) .....	28
Figure 3.1: The IKA MS-3 orbital shaker (left), Capintec CRC-25R (right).....	32
Figure 3.2: An AG50W-X series resin .....	33
Figure 3.3: Layout of separating column (left), close up of separating column (right) .....	36
Figure 4.1: Elution profile of $\text{Al}^{3+}/\text{Ga}^{3+}$ in 7 M HCl on Amberchrom CG71 column .....	45
Figure 4.2: Elution profile of $\text{Fe}^{3+}/\text{Ga}^{3+}$ in 7 M HCl on Amberchrom CG71 column .....	45
Figure 4.3: Elution profile of $\text{Zn}^{2+}/\text{Ga}^{3+}$ in 7 M HCl on Amberchrom CG71 column.....	47
Figure 4.4: Elution profile of $\text{Ge}^{4+}/\text{Ga}^{3+}$ in 7 M HCl on Amberchrom CG71 column .....	47
Figure 4.5: Elution profile of $\text{Sn}^{4+}/\text{Ga}^{3+}$ in 7 M HCl on Amberchrom CG71 column.....	48
Figure 4.6: Layout of radiolabelling method.....	50
Figure 4.7: First of five column separations of ions on Amberchrom CG71 column.....	52
Figure 4.8: Second of five column separations of ions on Amberchrom CG71 column ....	52
Figure 4.9: Third of five column separations of ions on Amberchrom CG71 column .....	54
Figure 4.10: Fourth of five column separations of ions on Amberchrom CG71 column ...	54
Figure 4.11: Fifth of five column separations of ions on Amberchrom CG71 column .....	55
Figure 4.12: A column separation of a $^{68}\text{Ga}$ spike from Ge, Sn, Fe and Zn.....	57



# Chapter 1

## Introduction

Positron emission particle tracking (PEPT) is a well-established technique which is applied to the non-invasive study of systems of flow, including fluid and granular flow in multiphase systems such as granulators, rotating kilns and ball mills (Parker and Fan, 2008). The technique was developed originally by Hawkesworth *et al.* (1986) with further development (Parker *et al.*, 1993) at the University of Birmingham, UK, resulting in the establishment of their Positron Imaging Centre. A new PEPT facility was then established in 2009 at iThemba LABS, South Africa (Buffler *et al.*, 2010).

A crucial aspect of the technique is the production of a suitable tracer particle. The tracer should be labelled with activity of an appropriate positron-emitting radionuclide and be representative of the particulate system under study in terms of size, shape and density. Some radionuclides used for PEPT are  $^{18}\text{F}$ ,  $^{61}\text{Cu}$ ,  $^{64}\text{Cu}$ ,  $^{66}\text{Ga}$  and  $^{68}\text{Ga}$ , as they decay by positron emission but have half-lives short enough to limit the dose to PEPT technique users and prevent the production of long-lived radioactive waste (Buffler *et al.*, 2010). In a PEPT experiment the tracer emits positrons, which annihilate with surrounding electrons to produce pairs of nearly back-to-back 511 keV gamma rays. These pairs of gamma rays penetrate through the system under investigation and may be detected in coincidence by the Positron emission tomography (PET) scanner. A virtual “line of response” thus

indicates the line along which the annihilation event has occurred. If multiple events are recorded in a short time, then the location of the tracer can be triangulated.

The two most established methods for tracer fabrication are: (1) direct activation of oxide containing materials (“direct activation”); and (2) the radiolabelling of ion exchange resins (“ion exchange”). In the current implementation of direct activation at the University of Birmingham, oxide-bearing tracer materials are bombarded with a  $^3\text{He}$  cyclotron beam to convert  $^{16}\text{O}$  in the tracer to  $^{18}\text{F}$  via the reaction  $^{16}\text{O}(^3\text{He},\text{p})^{18}\text{F}$ . The material must contain oxides and be thermally stable to withstand the high temperatures during bombardment. In practice, only tracers larger than  $\pm 1$  mm can be fabricated in this way.

The ion exchange method involves the radiolabelling of an ion exchange resin with a suitable positron-emitting radionuclide. Ion exchange is a reversible exchange of ions in a solution with ions on an immobile surface. Ion exchange materials are available in a wide range of forms for industrial processes based on the purification, separation or concentration of ions. A typical tracer fabrication by ion exchange involves evaporating a  $^{68}\text{Ga}$  eluate, supplied by a  $^{68}\text{Ge}/^{68}\text{Ga}$  generator, to dryness before re-dissolving the  $^{68}\text{Ga}$  in dilute hydrochloric acid in order to reduce the acidity. The solution is then left to equilibrate under mechanical shaking in a vial containing a particular cation exchange resin. During the equilibration process,  $^{68}\text{Ga}$  is sorbed from the solution before exchanging ions with the immobile surface.

Ion exchange resins can sorb substantial amounts of radionuclides such as  $^{18}\text{F}$  and  $^{68}\text{Ga}$ , making them a viable alternative to directly activated tracers. They are commercially available in a wide range of sizes (10-1200  $\mu\text{m}$ ), which makes them suitable for PEPT studies of fine granular systems. The most commonly-used ion exchange resins are manufactured from divinylbenzene crosslinked with styrene polymers, including NRW 100 and AG50W-X4, which are commercial organic cation exchange resins used at PEPT Cape Town. The polymer type and structure of NRW 100 and AG50W-X4 produce tracers with different physical and chemical properties from those of the granular systems of interest, such as in mineral processing: for example, NRW 100 has a specific gravity of approximately 1.1 which is lower than that of most metallic minerals. Nevertheless, tracers can be made to be more representative of the bulk by inserting them into larger particles (“drill and fill”), or by adhering a coating of the bulk material under investigation

to the surface of the tracers. The ion exchange method shows great practical application for PEPT due to the high levels of activity that can be labelled onto small tracers (Fan *et al.*, 2006a).

The PEPT Cape Town facility is located at iThemba LABS in Faure, South Africa which is licenced for producing and handling radionuclides. At PEPT Cape Town the main radionuclide used is  $^{68}\text{Ga}$ . It has a half-life that is long enough to obtain PEPT data over 3 hours of a typical experiment, yet short enough to decay to safe levels within 24 hours. This avoids the accumulation of costly and environmentally harmful radioactive waste, and reduces the radiation dose received by experimentalists from exposure to gamma rays.

$^{68}\text{Ga}$  is commercially available from a  $\text{SnO}_2$   $^{68}\text{Ge}/^{68}\text{Ga}$  generator, which comprises of a small column packed with specially treated  $\text{SnO}_2$  in a lead shield housing. The column is loaded with  $^{68}\text{Ge}$  which decays to  $^{68}\text{Ga}$  by electron capture. The amount of  $^{68}\text{Ga}$  produced is proportional to the amount of  $^{68}\text{Ge}$ , once both radionuclides are in equilibrium. The column is maintained under specific chemical conditions to strongly retain the  $^{68}\text{Ge}$ , and to enable the chemical separation of  $^{68}\text{Ga}$  by elution. Despite an equilibration time of approximately 14 hours between  $^{68}\text{Ge}$  and  $^{68}\text{Ga}$ , the generator can be eluted twice daily, as it takes only 4 hours to obtain 90% of the  $^{68}\text{Ga}$  potentially available.

Unfortunately,  $\text{SnO}_2$   $^{68}\text{Ge}/^{68}\text{Ga}$  generators degrade over time, having an effective lifespan of 6-9 months before significant amounts of  $^{68}\text{Ge}$  ions break through the column. As the generators degrade, they release increasing amounts of metal contaminants such as  $\text{Ge}^{4+}$  and  $\text{Sn}^{4+}$ . The release of  $\text{Ge}^{4+}$  is the result of  $^{68}\text{Ge}$  being dislodged from the  $\text{SnO}_2$  column, which also degrades over time releasing  $\text{Sn}^{4+}$  into solution. A significant amount of  $\text{Fe}^{3+}$  is found in the eluate and believed to be the result of environmental contamination, while the release of  $\text{Zn}^{2+}$  is the result of  $^{68}\text{Ga}$  decaying continually to stable zinc. The presence of these contaminants prevents consistent tracer labelling, as these metal contaminants may compete with  $^{68}\text{Ga}$  for ion exchange sites on the resin. This process is known as selectivity, and is determined by several factors which include the speciation of the ion, the counter ion, the exchange site and the material and structure of the ion exchange resin.

$^{68}\text{Ge}/^{68}\text{Ga}$  generators are expensive and have the potential to produce significant amounts of  $^{68}\text{Ga}$  beyond their recommended lifespan. This work will investigate whether the

lifespan of a  $^{68}\text{Ge}/^{68}\text{Ga}$  generator can be extended by removing the contaminants from the  $^{68}\text{Ga}$  eluent supplied by the  $\text{SnO}_2$   $^{68}\text{Ge}/^{68}\text{Ga}$  generator. This should reduce the competition for exchange sites on the selected cation exchange resins for sufficient sorption of  $^{68}\text{Ga}$ . This should save the enterprise significant costs, and could also improve the performance of the current radiolabelling process, with the potential to radiolabel smaller ion exchange resins with sufficient activity for PEPT measurement which, in turn, has the potential to increase the range of applications of the PEPT technique.

## **1.1 Research objectives, questions and scope**

### **1.1.1 Objectives**

The objectives of this work are thus the following:

1. To determine the selectivity of  $\text{Ge}^{4+}$ ,  $\text{Sn}^{4+}$ ,  $\text{Ga}^{3+}$ ,  $\text{Fe}^{3+}$ ,  $\text{Al}^{3+}$ ,  $\text{Ti}^{3+}$  and  $\text{Zn}^{2+}$  on the ion exchange resins NRW 100 and AG50W-X4 currently used at PEPT Cape Town.
2. To test and improve a  $^{68}\text{Ga}$  purification method using Amberchrom CG71 chromatographic resin to remove the contaminants inherent to  $\text{SnO}_2$   $^{68}\text{Ge}/^{68}\text{Ga}$  generators, to produce a standard procedure that is consistent and repeatable.
3. To compare the radiolabelling performance of the purified  $^{68}\text{Ga}$  eluate with the current method used at PEPT Cape Town, to determine the effect of the purification process. As quantitative analytical methods for determining  $^{68}\text{Ga}$  purity are unfeasible, a comparison study using radiolabelling performance of the current radiolabelling will be used instead.

### **1.1.2 Hypotheses**

The contaminant ions present in the eluate from a 1-year-old  $\text{SnO}_2$   $^{68}\text{Ge}/^{68}\text{Ga}$  generator compete with  $^{68}\text{Ga}$  for exchange sites on the NRW 100 and AG50W-X4 cation exchange resins currently used at PEPT Cape Town and can be removed within sufficient time to permit the use of  $^{68}\text{Ga}$  in PEPT studies within its period of radioactive decay. Purifying the  $^{68}\text{Ga}$  eluent will increase both the amount radiolabelled and the consistency of tracer

particle production used for PEPT studies. The lifespan of  $\text{SnO}_2$   $^{68}\text{Ge}/^{68}\text{Ga}$  generators will increase beyond the current 6 to 9 month limit.

### 1.1.3 Scope

The organic cation exchange resins chosen for use in this work are the strongly acidic cation exchange resins NRW 100 and AG50W-X4, which were determined in previous studies (van Heerden, 2010, 2012) as having a high selectivity for  $^{68}\text{Ga}$ , sufficiently rapid chemical sorption, and a high exchange capacity. The selectivity of NRW 100 and AG50W-X4 for each contaminant will be determined before performing column separations between each contaminant and  $^{68}\text{Ga}$ . By determining the extent of competition between  $^{68}\text{Ga}$  and the competing contaminant ion, the degree of interference in the radiolabelling method can be determined. By purifying  $^{68}\text{Ga}$  with the modified separation method, the lifespan of the  $^{68}\text{Ge}/^{68}\text{Ga}$  generator can be extended to radiolabel  $^{68}\text{Ga}$  on NRW 100 and AG50W-X4 consistently.

### 1.1.4 Key questions

The research questions for this work will be as follows:

1. How can the eluent from an aged  $\text{SnO}_2$   $^{68}\text{Ge}/^{68}\text{Ga}$  generator be purified to produce consistent radiolabelling on cation exchange resins? For example, a suitable target would be to radiolabel at least 1.0 mCi of  $^{68}\text{Ga}$  to a 465  $\mu\text{m}$  diameter NRW 100 resin bead.
2. How can the lifetime of a generator be extended beyond the expected lifespan of 6-9 months without adding significant process time?

## 1.2 Organisation of thesis

The remainder of this thesis commences with a review of the published literature relevant to the work in this study, starting with a description of the phenomenon of positron decay used in positron emission tomography (PET) and positron emission particle tracking (PEPT). The PEPT technique is then discussed in detail together with a description of the PEPT Cape Town facility and PET scanner. The different tracer-manufacturing techniques are discussed before focus is placed on the ion exchange technique, which is the method of production used at PEPT Cape Town. The properties and ion exchange resins relevant to the production of tracers for PEPT studies are then reviewed. Next, the  $^{68}\text{Ga}$  supply and associated issues concerning the radiolabelling process are discussed before a report of the state of the art of gallium purification techniques using ion exchange technology is given. Chapter 2 ends with a statement of the research objectives, hypotheses, scope and key questions.

Chapter 3 describes the equipment, materials and experimental methods used in this study. The methods for resin and resin column preparation are then listed before a definition of these methods is given.

Chapter 4 presents the results, followed by a discussion of the tests reported in Chapter 3, in the same order as those described in Chapter 3.

The conclusion of this work is given in Chapter 5, before listing recommendations for future work which could further improve the purification method and radiolabelling technique.

# Chapter 2

## Radionuclides for PEPT

This chapter will introduce positron emission particle tracking (PEPT) and the components required to use the technique successfully. The chapter begins with a description of the type of radionuclide required, followed by how the technique works. A detailed discussion of the tracers required for use in PEPT, and the methods to make them, are then discussed. Finally, the radionuclide supply for a preferred tracer production method is discussed.

### 2.1 Positron decay

Unstable isotopes are either in excess or deficient of neutrons, which leads to nuclear decay in order to obtain stability. Nuclear decay occurs through alpha, beta or gamma decay, with each isotope undergoing its own decay chain. Isotopes which have neutron deficient nuclei undergo beta decay ( $\beta^+$ ) and produce positrons: for example, the  $\beta^+$  decay

of  $^{11}\text{C}$  (Equation 2.1) emits a fast positron and an electron neutrino, and forms the new stable isotope  $^{11}\text{B}$ :



Positrons with high velocity travel only a short distance before they collide with electrons in surrounding matter (Phelps *et al.*, 1975). The positrons lose kinetic energy in these collisions with electrons before annihilation. The positron-electron annihilation results in the emission of a pair of nearly back-to-back 511 keV gamma rays (Figure 2.1). The energy of these gamma rays is equivalent to the combined rest masses of electron and positron in order to conserve momentum (Anderson *et al.*, 1999).

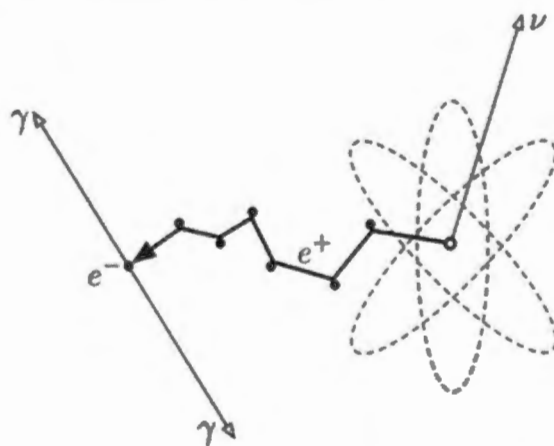


**Figure 2.1: Illustration of the decay path of a positron emitted via  $\beta^+$  decay**

## 2.2 Positron emission particle tracking

PET is used predominantly as a medical tool to image organs non-invasively by the controlled sorption of a radionuclide to the target organ. As mentioned above, positrons that originate from the tracer radionuclide annihilate with local electrons and produce back-to-back gamma ray pairs (Levin and Hoffman, 1999). If both back-to-back gamma rays from each annihilation event are detected in coincidence by two detector blocks, a virtual line of response (LOR) can be formed between these blocks. The LOR indicates the range of potential origins of the annihilation event. Multiple LORs can be used to reconstruct an image of the distribution and concentration of the tracer in the subject. A drawback is that some of the generated LORs may be corrupted either through deflection

of a gamma ray by Compton scattering in the subject material, or the coincident detection of two gamma rays from different positron annihilations.

While PET data is used to produce a three-dimensional map of the tracer in the patient, PEPT data is analysed in a markedly different way. PEPT data analysis focuses on locating the centroid of the tracer by triangulation, as opposed to imaging the shape, size and location of the tracer as required by PET. Although PEPT also uses the LORs detected by a PET scanner, the centroid of a single-point positron-emitting tracer particle is calculated, and a trajectory of the particle within the system under study is built (Figure 2.2). PEPT was devised at the University of Birmingham in the 1980s (Hawkesworth *et al.*, 1986); later, Parker *et al.* (1993) developed the triangulation technique to bin the LORs into small time steps, of the order of 1 ms. This bin size,  $N$ , can range from a minimum of three LORs up to several hundred. Within each bin, an iterative algorithm triangulates the tracer location by finding the set of LORs in each bin that intersect within the closest range. In this way, a final fraction of LORs,  $f$ , is obtained and the corrupt LORs discarded. This method can track the tracer location with a frequency of up to 1 kHz to a spatial resolution of 1 mm (Wildman and Parker, 2002). The spatial resolution is limited by the finite range of the positron in the system, the size of the tracer, and a small acollinearity in the back-to-back gamma rays, which is around  $0.2^\circ$  (Moses, 2011).

An addition to the field of PEPT was made in August 2009 with the opening of a dedicated PEPT facility, namely PEPT Cape Town, and the installation of an “EXACT3D HR++ PET scanner (model:CTI/Siemens 966)”. This camera contains a cylindrical orientation of detector cells with 820 mm diameter and axial length of 234 mm for maximum sensitivity (Figure 2.3). The scanner can sustain a list mode data acquisition rate of over 4 million events per second (4 MHz). The EXACT3D HR++ was designed to have superior resolution and sensitivity with a total of 27648 bismuth germinate oxide detector cells (Spinks *et al.*, 2000). This high resolution and sensitivity is of great benefit to PEPT Cape Town, as the camera is able to locate the position and velocity of a tracer with less than  $20 \mu\text{Ci}$  ( $7.4 \times 10^5 \text{ Bq}$ ) of radioactivity in a low attenuation environment (Cole *et al.*, 2012).

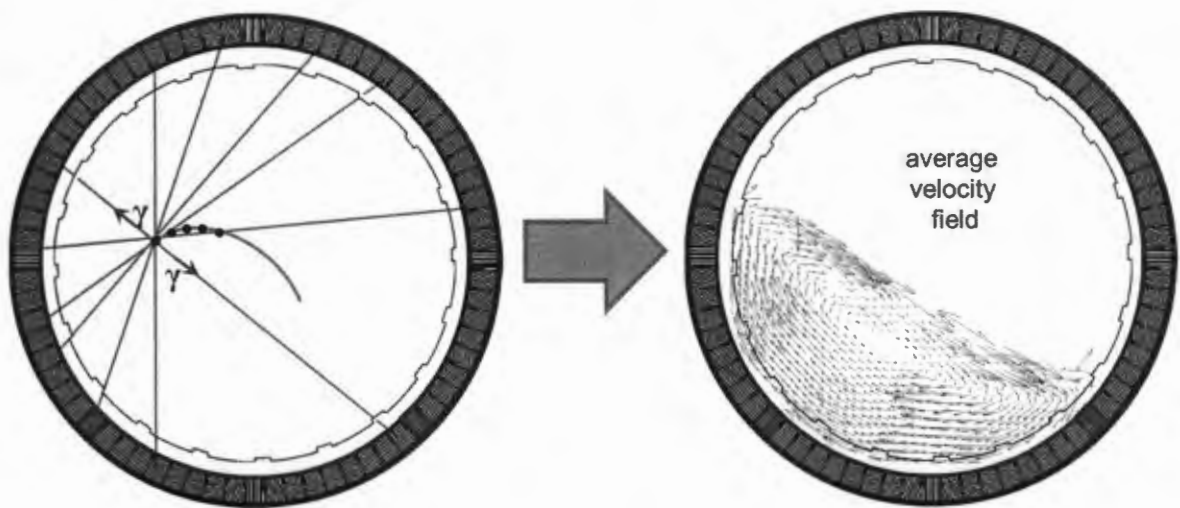


**Figure 2.2: The gamma rays detected by the PET scanner (grey ring) in coincidence from the resulting positron annihilation are generated as LORs (red lines) and used for triangulating the position of the tracer (black dot). Given sufficient tracer locations and data processing, valuable information, such as the average velocity field of a tumbling mill grinding media, can be determined (right).**

Many systems employing PEPT contain materials with high attenuation for 511 keV gamma rays, which can be overcome by labelling a higher initial activity on the tracer to ensure that sufficient LORs are detected to triangulate the tracer location. Cole *et al.* (2013) estimated a lower limit of 150  $\mu\text{Ci}$  for tracer particles moving at an average velocity of  $3 \text{ m}\cdot\text{s}^{-1}$ , in order to sustain a PEPT tracking frequency of 1 kHz and accuracy of  $\pm 1 \text{ mm}$ . As exposure to radiation poses an indeterminate risk of harm to users, an upper limit of 1000-1500  $\mu\text{Ci}$  per tracer has been imposed on the PEPT Cape Town facility, with a practical working obligation to minimise the amount of activity required. The main radionuclide used at PEPT Cape Town is  $^{68}\text{Ga}$ , which has a half-life of 68 minutes. An upper limit of 1500  $\mu\text{Ci}$  allows 3 hours of data collection on average before reaching the lower limit of 160-240  $\mu\text{Ci}$ . The supply of  $^{68}\text{Ga}$  radionuclide allows for tracer production twice daily at PEPT Cape Town, which enables as much as 6 hours of tracking time.

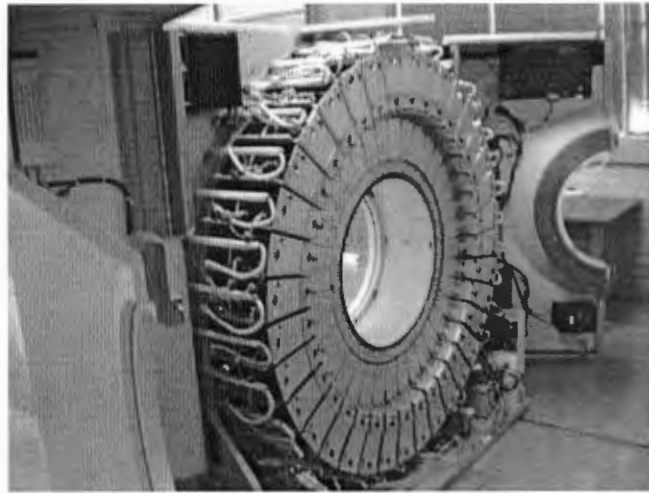


**Figure 2.3: The inside of the Siemens ECAD “EXACT3D HR++” PET scanner located at PEPT Cape Town.**

PEPT Cape Town is based at the South African government facility iThemba Laboratories for Accelerator Based Sciences (LABS) in Faure, Cape Town. The laboratories are used for the development and research of atomic sciences and associated technologies, which can be categorised further into four sections: research, radionuclide production, medical radiation and community interaction and training. The tracer production laboratory is situated within the Radionuclide Production Department (RPD) responsible for the production and supply of isotopes to industry and nuclear medicine centres in South Africa. The Department produces several radionuclides, namely,  $^{123}\text{I}$ ,  $^{67}\text{Ga}$ ,  $^{81}\text{Rb}$ ,  $^{18}\text{F}$ ,  $^{22}\text{Na}$ ,  $^{68}\text{Ge}$ ,  $^{82}\text{Sr}$  and  $^{88}\text{Y}$  by proton bombardment supplied by a 200 MeV Separate Sector Cyclotron (van der Meulen, 2008). Of the aforementioned radionuclides, only  $^{18}\text{F}$ ,  $^{22}\text{Na}$ ,  $^{68}\text{Ga}$  (via decay from  $^{68}\text{Ge}$ ), and  $^{82}\text{Rb}$  (via decay from  $^{82}\text{Sr}$ ) are positron emitters (iThemba Laboratory for Accelerator Based Sciences, radionuclides, 2013; IAEA-DCRP, 2006). These neutron-deficient radionuclides have different half-lives, with  $^{68}\text{Ga}$  ( $t_{1/2} = 68$  min) and  $^{18}\text{F}$  ( $t_{1/2} = 108$  min) having the greatest availability and practical use for PEPT studies.  $^{68}\text{Ga}$  is readily available from a  $^{68}\text{Ge}/^{68}\text{Ga}$  generator and, along with  $^{18}\text{F}$ , has a sufficiently short half-life to prevent the possibility of producing long-lived radioactive waste.

## 2.3 Production of tracers for PEPT

PEPT tracers are a crucial part of the PEPT technique, as the reliability of the data output from a PEPT study is dependent on how representative the physical characteristics of the tracers are to the media under study. If the tracer is not made to represent the media under study then the PEPT data could show the behaviour of the tracer in the media. The tracer is also required to emit a sufficient number of positrons to be located accurately in an opaque system. If the tracer does not satisfy these requirements, the PEPT technique cannot be implemented successfully. There are two methods of tracer production that have been used repeatedly in PEPT studies: direct activation and chemical sorption (Table 2.1). Chemical sorption is further divided into surface modification and ion exchange radiolabelling. Radiolabelling is a process where a radionuclide displaces ions bound to the exchange sites of an ion-exchange resin. Drill and fill is a method of tracer manufacture that introduces a small tracer into a larger particle. The following section will review the methods commonly used for producing tracers for PEPT studies.

**Table 2.1: Summary of the different types of PEPT tracers**

	Direct activation	Chemical sorption	
		Surface	Ion exchange
Requirements	Cyclotron	Positron supply	Positron supply
Typical size range [ $\mu\text{m}$ ]	>1000	None	50-1200
Typical material	Contain oxides	reacts with positron	Ion exchange
Typical activity [ $\mu\text{Ci}$ ]	2 600*	+/-600	800-1000

\*Activity for size range greater than 1 mm instead of 212-250  $\mu\text{m}$ .

### 2.3.1 Tracers produced by the direct activation method

The method of direct activation features the bombardment of either  $^{16}\text{O}$  with  $^3\text{He}$  or  $^{18}\text{O}$  with protons in a cyclotron to create  $^{18}\text{F}$ . For example, the University of Birmingham uses a  $^3\text{He}$  beam supplied by a 33 MeV MC40 cyclotron irradiates  $^{16}\text{O}$  containing oxides to

produce  $^{18}\text{F}$  through the nuclear reaction  $^{16}\text{O} (^3\text{He,p}) ^{18}\text{F}$ . The material being irradiated needs to contain the appropriate oxides and be stable thermally. The oxide material needs to be larger than 1 mm in diameter for sufficient activity to be used in a PEPT experiment.

Many PEPT studies have been performed successfully with tracers made through direct activation, by bombarding silica-based tracers of appropriate size in the form of glass (Parker *et al.*, 1997; Laurent *et al.*, 2002; Stein *et al.*, 2002; Bbosa *et al.*, 2011) or sand particles (Kuo *et al.*, 2003; Griffiths *et al.*, 2008). Less frequently used oxygen containing tracer materials such as alumina (Griffiths *et al.*, 2008) and ceramics (van der Westhuizen *et al.*, 2011) have also been used for PEPT studies. This latter method is not limited to  $^{18}\text{F}$  production, as Stellema *et al.*, (1998) used direct activation of  $\text{CuO}_2$ -impregnated glass beads to produce  $^{64}\text{Cu}$  tracers. The application of direct activation for tracer fabrication is limited ultimately by the type of tracer material required and the costly operation of a cyclotron.

### 2.3.2 Tracers produced by chemical sorption methods

Surface modification either requires a material which naturally sorbs the target isotope or relies on making the material surface react with the target isotope. One of the major advantages of the surface modification method is that  $^{18}\text{F}$  can be labelled directly onto the surface of materials without a restriction on size or cross-sectional area. Tracer materials that have been modified successfully include rounded sand (Chan *et al.*, 2009; Chan *et al.*, 2009), glass (Cole *et al.*, 2010; Griffiths *et al.*, 2011), alumina (Griffiths *et al.*, 2011), MCC (Depypere *et al.*, 2009), unmodified synthetic and natural pyrites (Waters *et al.*, 2008), and even radish seeds (Van de Velden *et al.*, 2008), with diameters varying from 2.5 mm down to 70 microns.

Ion exchange radiolabelling relies on controlling the uptake of a desired radionuclide by an organic ion exchange resin. The tracers produced are typically not representative of the particles of interest, but may be made so by two methods. The coating method uses ion exchange resins which can be coated to modify the surface properties (Cole *et al.* 2014) or density to suit those of the particle of interest. The “drill and fill” method, described in section 2.3.3 below, applies for larger particles.

The tracer production method routinely used at PEPT Cape Town uses strongly acidic cation exchange resins radiolabelled with  $^{68}\text{Ga}$  in dilute hydrochloric acid. It was developed previously at PEPT Cape Town by the author (van Heerden, 2012) and will be described as the “standard” radiolabelling procedure, as it is used every day at PEPT Cape Town to ensure the production of tracer particles labelled with a consistent amount of  $^{68}\text{Ga}$ . The current ion exchange resins selected for use in the “standard” radiolabelling procedure are NRW100 and AG50W-X4. Both strongly acidic cation exchange resins are made of an organic polymer matrix and sulfonic acid exchange sites. The effectiveness of the “standard” radiolabelling forms a critical component of this work and improvement of such adds substantial value to the enterprise. The procedure is as follows:

An  $\text{SnO}_2$   $^{68}\text{Ge}/^{68}\text{Ga}$  generator (such as that typically available at iThemba LABS’ Radionuclide Production Department) is eluted with 4.5 ml of 0.6 M HCl to obtain a supply of  $^{68}\text{Ga}$ , of which the first 1.0 ml is discarded, as the initial dead volume contains no  $^{68}\text{Ga}$ , only contaminants. The dead volume is a result of 0.6 M HCl filling the outlet tube. The remaining 3.5 ml of  $^{68}\text{Ga}$  in 0.6 M HCl eluent is decanted into a 200 ml Teflon beaker which has been pre-heated briefly to 250°C (Figure 2.4, 1). The beaker is pre-heated in order to reduce the time required for evaporation. The eluate is evaporated to dryness over a 25-35 minute period before being re-dissolved in 300  $\mu\text{L}$  of 0.005 M HCl, which is added by means of a syringe (Figure 2.4, 2). This step ensures that the pH ranges from 3 to 7, so that the  $^{68}\text{Ga}$  solution will have preferable radiolabelling conditions for the NRW 100 and AG50W-X4 cation exchange resins typically used for PEPT studies at PEPT Cape Town.

The  $^{68}\text{Ga}$  solution is then added to a small vial containing between 2 and 4 strongly acidic cation exchange resin beads, with a diameter of  $475\pm 10$   $\mu\text{m}$  each (Figure 2.4, 3). This resin bead diameter was selected based on the most abundant of the smallest size of NRW 100, as the resin is produced across a range of only 425–1200  $\mu\text{m}$  in diameter. Several ion exchange resin beads are added to the vial to improve the reliability of the procedure.

The vial is sealed and placed on an orbital shaker for 30 minutes to sorb  $^{68}\text{Ga}$  (Figure 2.4, 4). The time required for radiolabelling  $^{68}\text{Ga}$  on the orbital shaker depends on the size of the resin beads and the desired amount of activity. The smaller resin beads have a shorter

equilibrium time than their larger counterparts, and also have a lower capacity. At the conclusion of the shaking process, the resin beads are removed from the solution and placed into individual vials before their radiolabelled activity is measured in an ionisation chamber.

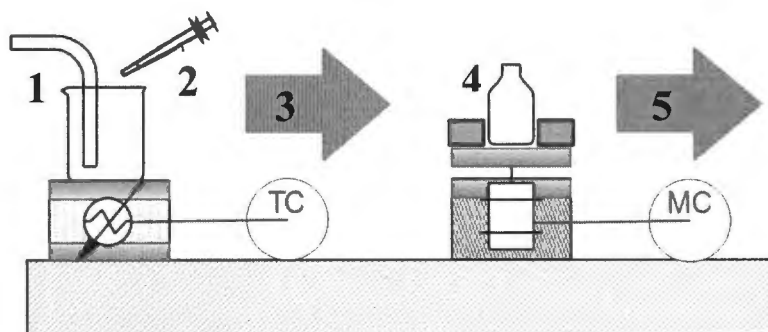


**Figure 2.4: Overview of the standard radiolabelling procedure. (1) corresponds to the Teflon beaker while (2) illustrates the syringe used to dispense 0.005 M HCl. The arrow labelled (3) represents the addition of resin beads and re-dissolved  $^{68}\text{Ga}$  added to the vial labelled (4), after which the activity is measured in an ionization chamber (5).**

The total time required to complete the radiolabelling process is approximately 50-75 minutes. For NRW100 ion exchange resin beads larger than 300  $\mu\text{m}$  in diameter, the process yields at least 500  $\mu\text{Ci}$   $^{68}\text{Ga}$  activity per resin bead for a 30 mCi  $\text{SnO}_2$   $^{68}\text{Ge}/^{68}\text{Ga}$  generator radionuclide supply over a period of 1 year.

### 2.3.3 Tracers produced by the “drill and fill” method

The “drill and fill” method of tracer production requires that a particle intended for tracking with PEPT is large and rigid enough not to break while being drilled to the centroid. The bottom of the drilled hole is then filled with the selected positron-emitting radionuclide before being sealed with an appropriate epoxy (Figure 2.5). The application of direct activation for tracer fabrication is limited ultimately by the type of tracer material required and the costly operation of a cyclotron for irradiation. This makes the “drill and fill” method a viable alternative for PEPT applications, where radionuclides can be obtained without the need for a cyclotron.

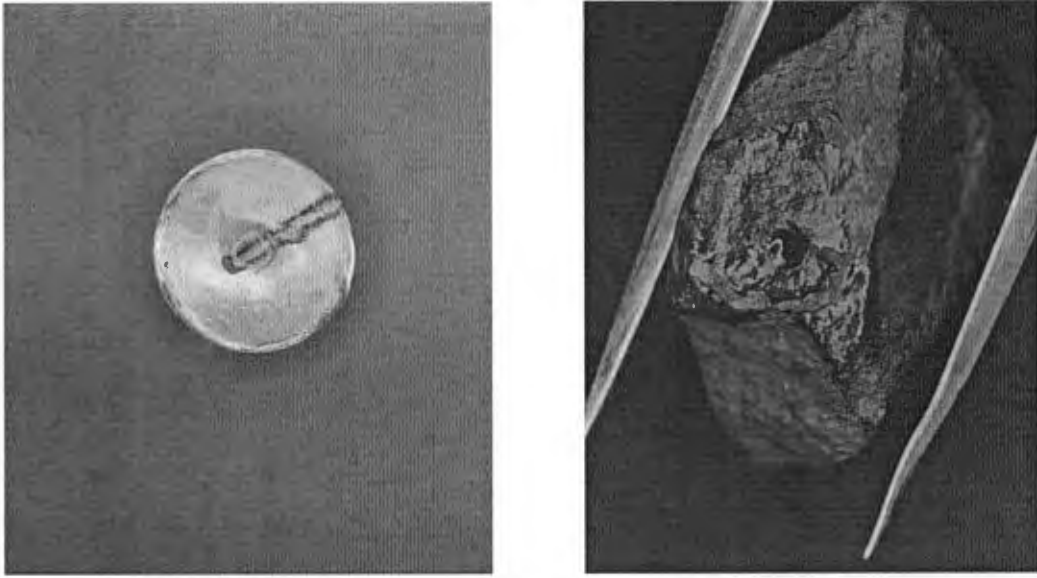


**Figure 2.5: Two examples of the "drill and fill" method, using an 8 mm glass bead (left) and haematite chip (right) sealed for use as PEPT tracers**

## **2.4 Properties of ion exchange resins**

Ion exchange is a process of exchanging counter-ions reversibly on oppositely-charged immobile ions. Ion exchange materials are available as a wide range of different polymer forms; ion exchange resins are predominantly made of organic polymers, and are produced commercially with a wide range of physical and chemical properties to suit many applications. Commercial suppliers characterise the chemical and physical properties of ion exchange resins to help determine the desired combination of properties for a specific application. The ideal resin properties are: fast chemical kinetics; high chemical, physical and mechanical stability; hydrophilic surface behaviour; highly reactive functional groups with the ability to regenerate; consistent particle size and form and a large surface area.

Ion exchange resins with negatively-charged immobile ions have positively-charged counter-ions available for exchange. These resins may be classified as cationic exchange resins, and can be split into three main groups: strong acid, mild acid and weak acid (ion exchangers). Strong acid cation exchange resins such as NRW 100 and AG50W-X4 share the chemical behaviour of a strong acid. The immobile ions for both strong acid cation exchange resins are sulphonic acid groups. Figure 2.6 illustrates an example of a strong acid cation exchanger exchanging a hydrogen counter-ion with a sodium counter-ion.

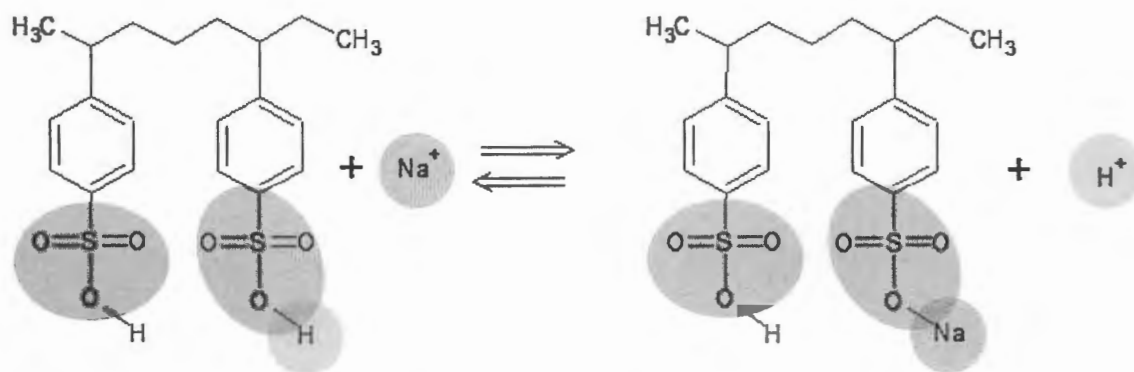


**Figure 2.6: Illustration of a cationic exchange resin with sulphonic acid functional groups (red) exchanging a hydrogen counter-ion (green) for a dissolved sodium ion (blue)**

The following subsections describe the measurable chemical properties of ion exchange resins used to gauge the suitability of a particular ion exchange resin for the desired application.

### 2.4.1 Exchange capacity

For every active exchange site in an ion exchange material, an equivalent counter-ion is present to balance the charge. Therefore, the exchange capacity of a resin is a measure of active counter-ion equivalents that can be sorbed in a unit mass of ion exchange material. Exchange capacity can be measured under static or dynamic conditions. Static exchange capacity can be regarded as a batch process where the amount of solute and resin is fixed. Dynamic capacity is measured by passing the solute continually through a fixed amount of resin.

### 2.4.2 Equilibrium measurements for ion exchange resins

The ion exchange isotherm describes the sorption of ions on the surface of the ion exchange resin at equilibrium and under constant temperature conditions. The ion exchange isotherm can be expressed by equilibrium measurements. The equilibrium

measurements used in this work are: selectivity coefficients, equilibrium distribution coefficients and separation factors.

### *Selectivity coefficient*

The selectivity coefficient of an ion exchange resin is a measure of its ability to sorb one ionic species more than another, under equilibrium conditions. A simple equation of the selectivity of a cation exchange resin R for a metal ion  $A^+$  over the initial counter-ion  $H^+$  is shown below:



For a particular resin, selectivity is quantified by the selectivity coefficient and changes with operating conditions. The selectivity coefficient  $K_{H^+}^{A^+}$  is given by the equation:

$$K_{H^+}^{A^+} = \frac{[A^+]_R}{[H^+]_R} \cdot \frac{[H^+]_{soln'}}{[A^+]_{soln'}} \quad (2.3)$$

For strongly acidic and basic ion exchange resin at ambient conditions, the selectivities for hydrated ions are generally as follows (Kunin, 1951): higher valence ions are more preferable; the least hydrated ions are more preferable, and ions with the lowest tendencies to form complexes are more preferable. The trend for hydrated ionic radii is: the higher the atomic number, the lower the hydrated ionic radius.

### *Equilibrium distribution coefficients*

The equilibrium distribution coefficient is a measure of the ability of an ion exchange resin to remove an ionic specie from a solution. This measurement gives the allocation of ionic species in equilibrium between the ion exchange resin and solution. The equilibrium distribution coefficient is abbreviated as  $K_d$  and is defined as:

$$K_d = \frac{\text{mass of element in resin}}{\text{mass of element in solution}} \cdot \frac{\text{volume of solution}}{\text{mass of dry resin}} \quad (2.4)$$

Distribution coefficients are commonly used in ion exchange chromatography as they can be used to estimate the elution order in ionic separations (Smith-Jones and Strelow, 1986). Elution is a process of extracting one material from another by washing with a solvent.

For example, Badawy *et al.* (2009) determined the distribution coefficients of  $\text{Al}^3$ ,  $\text{Fe}^{3+}$ ,  $\text{Ba}^{2+}$  and  $\text{Pb}^{2+}$  on Purolite C100. Using the distribution coefficients, they were able to separate and recover environmentally-toxic Pb with a Purolite C100 column.

### ***The separation factor***

The separation factor is a value which indicates the preference of an ion exchange material for one of two counter-ions. This is expressed as the ratio of two distribution coefficients measured under identical operational conditions. The separation factor is defined as:

$$\alpha_A^B = \frac{K_d^B}{K_d^A} \quad (2.5)$$

As well as finding the distribution coefficients in the separation of Pb, Badawy *et al.* (2009) calculated the separation factors at the beginning of their experiments to evaluate whether the separation process was technically possible. A separation factor greater than 50 should give rapid and well separated sharp peaks from the elution profile, whereas separation factors below 1.3 mean that separation of the two ions is technically unfeasible.

### **2.4.3 Interactions of ion exchange materials**

In addition to the mechanism of ion exchange, other interactions can occur between the solute and the resin. These interactions may be employed to separate ionic species, to either add to or replace the ion exchange process. Some of the exchange mechanisms are capable of separating non-ionic species; the most relevant to this study being complex formation and non-exchange sorption.

#### ***Complex formation***

Ions can be separated by their ability to form ionic complexes, i.e. to bond with other molecules or ions called ligands. Some polyvalent ions have a stronger tendency to form complexes with surrounding ligands. The speciation of the polyvalent ion can be changed with the addition of charged ligands. For example,  $\text{Ga}^{3+}$  in an aqueous ionic solution will change from the hydrated specie to the chloro-complex species with the addition of

hydrochloric acid (Zhernosekov *et al.*, 2007; Sen *et al.*, 2011). A separation performed on a strong acid cation exchange resin in high hydrochloric acid concentrations causes the negatively charged  $\text{GaCl}_6^{3-}$  specie to have minimal resin interaction. Thus, the complex will be eluted before an ion that is less likely to form a chloro-complex.

### ***Non-exchange sorption***

Non-exchange sorption is the retention of ions and molecules, which can occur in addition to or instead of the ion exchange process. Non-exchange sorption can be divided into two types: stoichiometric and non-stoichiometric. Non-stoichiometric sorption interactions can occur with or instead of stoichiometric sorption. The most common of these interactions are sorption of electrolytes from concentrated solutions and sorption of large organic molecules by the resin surface. Organic molecule interactions and stoichiometric sorption are not applicable to this work. Chromatographic resins are able to separate ions or molecules using non-exchange sorption. Ions or molecules are thus separated by how strongly they are sorbed onto the resin surface as opposed to the use of ion exchange chromatography.

In electrolytic sorption, pairs of charge balanced cation-anions are transferred from the bulk solution to the internal solution. The amount transferred depends on the electrolyte concentration of the bulk solution and the operational conditions. The surface sorption does not depend on ion exchange capacity and is limited to the square area of the pore surface. The size and morphology of the sorped electrolytes will, along with other factors, determine the sorption capacity (Zagorondi, 2006).

### **2.4.4 Resins used at PEPT Cape Town**

The cation exchange resins NRW 100 and AG50W-X4 were chosen to be used in the radiolabelling process in a previous study (van Heerden, 2010). The chromatographic resin Amberchrom CG71 was considered for the separation method to remove the contaminants from gallium based on the works of Naidoo (1998) and Naidoo and van der Walt (2001).

### ***The resins NRW100 and AG50W***

PuroLite NRW100 is a strongly acidic cation exchange resin. The nuclear grade resin is designed for the purpose of removing radioactive isotopes from aqueous solution. The resin is a gel-like microporous resin structure that is made from polystyrene cross-linked with divinylbenzene. The resin beads are golden-dark brown spheres.

The AG50W series of resins are gel-like strong acid cation exchange resins. The resins are designed for analytical methods and are available in a range of cross-linking amounts, indicated with the suffix “X”, and a number relating to the percentage by mass of cross-linking agent used for the resin structure. AG50W-X2 and -X4 are designed for separating or concentrating peptides, nucleotides and amino acids. The AG50W-X8, -X12 and -X16 range of resins are designed for separating small peptides and amino acids, for cation removal from solutions and metal separations (Table 2.2).

Both NRW 100 and AG50W-X4 report good exchange capacities and high chemical and mechanical stability. Both resins are manufactured to have consistent shape and well screened sizes, as required by their aforementioned applications. Neither of the resins has data available on the effective surface area, but both have been proven adequate as PEPT tracers in preliminary studies (van Heerden, 2012). The high moisture retention of NRW 100 ensures that the resin is hydrophilic in nature. The combination of these properties has demonstrated that NRW 100 and AG50W-X4 are effective resins for use in PEPT studies.

### ***Amberchrom CG-71***

Amberchrom CG-71 is a chromatographic resin produced from a methylacrylate-based polymer. The resin is chemically stable with no active exchange sites and a high surface area (Table 2.2). The resin has a low degree of swelling as well as reproducible performance for reliable column stability. Amberchrom CG-71 resins are available in three size ranges, including a coarse range of 80-160  $\mu\text{m}$  which is used in this study. The large surface area and pore size give the resin the ability to operate at high flow rates. Amberchrom CG-71 has the chemical behaviour corresponding to non-exchange sorption as mentioned above in section 2.4.3. On occasion, chromatographic resins are able to separate ions of similar chemical behaviour, which ion exchange resins are typically not able to, as the technique does not require ionic interactions for separation (section 2.4.3).

**Table 2.2: Physical and chemical properties of select chromatographic and cation ion exchange resins**

	Cation exchange resins			chromatographic resin
<b>Resin name</b>	NRW100	AG50W-X4	AG50W-X8	Amberchrom CG-71
<b>Physical properties</b>				
Polymer material	Styrene	Styrene	Styrene	Methacrylate
Structure	Microporous	Microporous	Microporous	
% cross-link agent	unknown	4	8	7
Thermal stability [° C]	120	± 150	± 150	Unknown
Nominal density[kg/m <sup>3</sup> ]	1.2 <sup>a</sup>	0.8	0.8	1.28
Size range [µm]	425-1200	75-425	63-1180	80-160
<b>Chemical properties</b>				
Capacity [meq/ml]	1.8	1.1	1.7	Non-stoichiometric
Functional group	Sulfonic acid	Sulfonic acid	Sulfonic acid	None
Counter-ion	H <sup>+</sup> , hydrogen	H <sup>+</sup> , hydrogen	H <sup>+</sup> , hydrogen	None
Chemical stability [pH]	0-14	0-14	0-14	0-14
Predominant applications	Removing isotopes	Separating/ concentrating peptides.	Cations, Cation removal.	Chromatographic separations

<sup>a</sup> - specific gravity as opposed to nominal density

## 2.5 <sup>68</sup>Ga for ion exchange in PEPT

At PEPT Cape Town, <sup>68</sup>Ga is supplied by means of a SnO<sub>2</sub> <sup>68</sup>Ge/<sup>68</sup>Ga generator. A generator can be described as a self-contained system which contains a column housing a long-lived radionuclide (<sup>68</sup>Ge) that decays to a desired short-lived radionuclide (<sup>68</sup>Ga)

(Figure 2.7). The parent/daughter radionuclides are in equilibrium when the relative rate of  $^{68}\text{Ge}$  decay to  $^{68}\text{Ga}$  is in equilibrium with the amount of  $^{68}\text{Ga}$  present. Once in equilibrium, an operator can elute the short-lived radionuclide from the column, leaving behind the long-lived radionuclide. The column is made from a finely granulated porous  $\text{SnO}_2$  material that has a strong retention for  $^{68}\text{Ge}$  in dilute hydrochloric acid. The process can be repeated once equilibrium is achieved, thus creating a continual supply of the target radionuclide.

### 2.5.1 $\text{SnO}_2$ $^{68}\text{Ge}/^{68}\text{Ga}$ generators

$^{68}\text{Ge}/^{68}\text{Ga}$  generators are intended mostly for medical PET studies (Naidoo *et al.*, 2002). The ideal properties of a  $^{68}\text{Ge}/^{68}\text{Ga}$  generator include significantly different chemical properties between  $^{68}\text{Ge}$  and  $^{68}\text{Ga}$  with: a high separation factor ( $>50$ ) to enable easy elution of  $^{68}\text{Ga}$ ; an easily reproducible and operable generator design; a small elution volume with a high percentage  $^{68}\text{Ga}$  yield for a high concentration; a practical re-growth time from  $^{68}\text{Ge}$  to  $^{68}\text{Ga}$ , for the continual supply of  $^{68}\text{Ga}$  and longevity of  $^{68}\text{Ge}$ ; and no loss (breakthrough) of  $^{68}\text{Ge}$  through the lifespan of the generator which would reduce  $^{68}\text{Ga}$  yield and pose a serious contamination threat. In addition, the  $^{68}\text{Ga}$ -containing eluate should be chemically compatible for the desired purpose, and be shielded sufficiently to minimise the dose received by the operator.



**Figure 2.7: A cut-away example of a  $\text{SnO}_2$   $^{68}\text{Ge}/^{68}\text{Ga}$  generator (left), and  $\text{SnO}_2$   $^{68}\text{Ge}/^{68}\text{Ga}$  generators produced at iThemba LABS (right)**

Figure 2.7 shows an SnO<sub>2</sub> <sup>68</sup>Ge/<sup>68</sup>Ga generator with a cut-away section, revealing a small ion exchange column (highlighted in yellow rectangle), where the SnO<sub>2</sub> is contained between two sintered frits. The red area around the column indicates the lead shielding, while the two white caps above the column are the inlet and outlet ports.

## 2.5.2 Contaminants in an SnO<sub>2</sub> <sup>68</sup>Ge/<sup>68</sup>Ga generator

de Blois *et al.* (2011) studied SnO<sub>2</sub> <sup>68</sup>Ge/<sup>68</sup>Ga generators for the purpose of characterising and analysing the performance of radiolabelling DOTA-peptides for PET studies. From the semi-quantitative/qualitative analysis of the generator product they determined the presence of significant amounts of Sn, Fe and Zn contaminants (Table 2.3). The Sn and SnO<sub>2</sub> contaminants were from the SnO<sub>2</sub> column used in the <sup>68</sup>Ge/<sup>68</sup>Ga generator, which gradually degraded to release small amounts over time. From the amount of Fe present in the eluate, it was assumed to be an environmental contaminant which could interfere significantly in the labelling process (Zhernosekov *et al.*, 2007). Zn was also found in the eluate, owing to the decay of <sup>68</sup>Ga via positron emission:



The amount of Zn present in the eluate was found to depend on the time between two elutions (Table 2.3). The concentration of Zn exceeded the amount of <sup>68</sup>Ga present in a <sup>68</sup>Ge/<sup>68</sup>Ga generator within 3 hours (de Blois *et al.*, 2011). <sup>68</sup>Ge/<sup>68</sup>Ga generators can also be produced using an Al oxide-based column and, as such, the purification of these Al<sup>3+</sup> ions have been included in this study in an attempt to make the method compatible for most <sup>68</sup>Ga radionuclide generators. The amount of <sup>68</sup>Ge lost is reported as a percentage relative to the amount of <sup>68</sup>Ga present in the system, as the amount of <sup>68</sup>Ge installed in generators is not measured directly but rather by means of the amount of <sup>68</sup>Ga it can produce once in equilibrium. The eluate of a 10 μCi <sup>68</sup>Ge/<sup>68</sup>Ga generator was quantitatively analysed for <sup>68</sup>Ge break-through, tin, iron and zinc (Loch, 1980). A much higher activity 50 mCi <sup>68</sup>Ge/<sup>68</sup>Ga generator was later semi-quantitatively analysed for <sup>68</sup>Ge break-through and tin by McElvany *et al.* (1984).

**Table 2.3: Summary of reported contaminants of interest from  $^{68}\text{Ge}/^{68}\text{Ga}$  generators used for medical applications**

Article reference	$^{68}\text{Ge}$ Isotope		Elements [ppm]		
	Activity loaded	break-through	Sn	Fe	Zn*
De Blois <i>et al.</i> , 2011	10 mCi	< 0.001%	< 10	< 10	< 3
Loch, C., 1980	10 $\mu\text{Ci}$	< 0.0001%	0.42-0.54	0.16-0.18	0.12-0.16
McElvany <i>et al.</i> , 1984	50 mCi	< 0.003%	< 2	N/A	N/A

\*The amount of Zn present in a system is dependent on the time elapsed since the previous elution as  $^{68}\text{Ga}$  decays to  $^{nat}\text{Zn}$  and, as such, is also dependent on how much  $^{68}\text{Ge}$  is in the generator.

Closer examination of Table 2.3 reveals that no contaminant exceeded approximately 10 ppm. However, the total amount of  $^{68}\text{Ga}$  present in the system is typically of the order of  $10^{-9}$  to  $10^{-12}$  grams (14-0.014 ppb) meaning that the concentrations of the contaminants were typically far greater than those of  $^{68}\text{Ga}$ .

The selectivity of a species on a resin increases with increasing concentration; thus contaminants with a lower selectivity than  $^{68}\text{Ga}$  for NRW 100 and AG50W-X4 can be sorbed in larger amounts if present in higher concentrations. For efficient separations, the distribution coefficient of a target ion should be 50 times greater than the contaminants (section 2.4.2). In light of the presence of metal contaminants in the generator eluate, it is important to measure the selectivity of these ions on the ion exchange resins being used for PEPT applications in order to predict whether they will pose a problem with radiolabelling these resins with  $^{68}\text{Ga}$  as the generator ages. For neutral pH conditions in low ion concentration aqueous solutions, the trend for the order of affinity of cation exchange resins for metal ions is: the highest valence to lowest, the lowest hydrated ionic radius to highest, and from the least complex forming ion to the most complex (section 2.4.2). For the contaminants present in the eluate from  $^{68}\text{Ge}/^{68}\text{Ga}$  generators, the valences, ionic radii and ability to form complexes are reported in Table 2.4 (Greenwood and Earnshaw, 2006).

**Table 2.4: Physical properties of germanium, iron, gallium, tin and zinc in the chloride form (Greenwood and Earnshaw, 2006)**

Element	Co-ordination number [Cl]	Valence	Ionic radius [pm]
Germanium, <b>Ge</b>	6	4+	53
Iron, <b>Fe</b>	6	3+	55 (ls)*, 78 (hs)**
Gallium, <b>Ga</b>	6	3+	62.0
Tin, <b>Sn</b>		4+	118
Zinc, <b>Zn</b>		2+	74

\*ls - low spin electron configuration

\*\*hs – high spin electron configuration

The order of affinity for the aforementioned ambient pH conditions was deduced as follows:



Medical practitioners rely on pure radionuclides for effective radiolabelling of peptides for use in PET studies. Solutions can be treated beforehand with a purification step, or alternatively by synthesising a highly selective ion exchange resin, and/or adjusting the media in which the labelling occurs (i.e. adjusting the tendency to form complexes). Each of these methods has advantages and disadvantages, the largest contributing factor being time. There is no simple resin synthesis method which has superior selectivity of  $\text{Ga}^{3+}$  over  $\text{Ge}^{4+}$  and  $\text{Fe}^{3+}$ . Therefore, a  $^{68}\text{Ga}$  purification method developed by Naidoo (1998) and Naidoo and van der Walt (2001) was tested, and modified by integrating with the current radiolabelling method. Separating  $\text{Fe}^{3+}$  from  $\text{Ga}^{3+}$  is complicated because of the similarity in chemical properties, and because both ions share the same valence and similar ionic radii (Table 2.4), as described in subsection 2.4.2 (selectivity coefficient). Some methods have been developed for the medical industry to purify gallium isotopes to be used in radiolabelling DOTA-peptides and for radio-chemical separations in radionuclide

production. The labelling of DOTA-peptides with  $^{68}\text{Ga}$  improves after purification. Several methods of purification and separation are available, each of which is tailored for its specific use. A selection of available purification methods need to be examined for compatibility with the radiolabelling process. The most important factors for compatibility are the medium in which  $^{68}\text{Ga}$  is purified and the medium used to elute  $^{68}\text{Ga}$  from the column.

### 2.5.3 Methods to purify the $^{68}\text{Ga}$ eluate

Although gallium purification was not the focus of some of these methods, the data reported allows for development of a method. Strelow (1980) and Strelow and van der Walt (1987) performed quantitative separations of gallium using AG50W-X4 cation exchange resin and hydrobromic acid-acetone media. Both methods report high purity and recovery of gallium with small columns. In spite of these efficiencies, neither reports on how to remove  $\text{Sn}^{4+}$  and  $\text{Ge}^{4+}$  from  $\text{Ga}^{3+}$ . Furthermore, separations with hydrobromic acid are not suitable for the present work because of the formation of bromo-gallium complexes (which have an unknown effect on radiolabelling in PEPT), and to avoid producing waste more toxic than its chloride counterpart.

Strelow *et al.* (1965) investigated the selective elution of four of the elements of interest using the cation exchange resin AG MP50 in sulphuric and nitric acid media; they employed large columns and reported low separation factors (Figure 2.8, red/green). Strelow and Sondorp (1972) made use of perchloric acid media to reduce the possibility of complex formation when determining distribution coefficients on AG50W-X8. Strelow *et al.* (1965) reported slightly lower separation factors than Strelow and Sondorp (1972) for Zn.

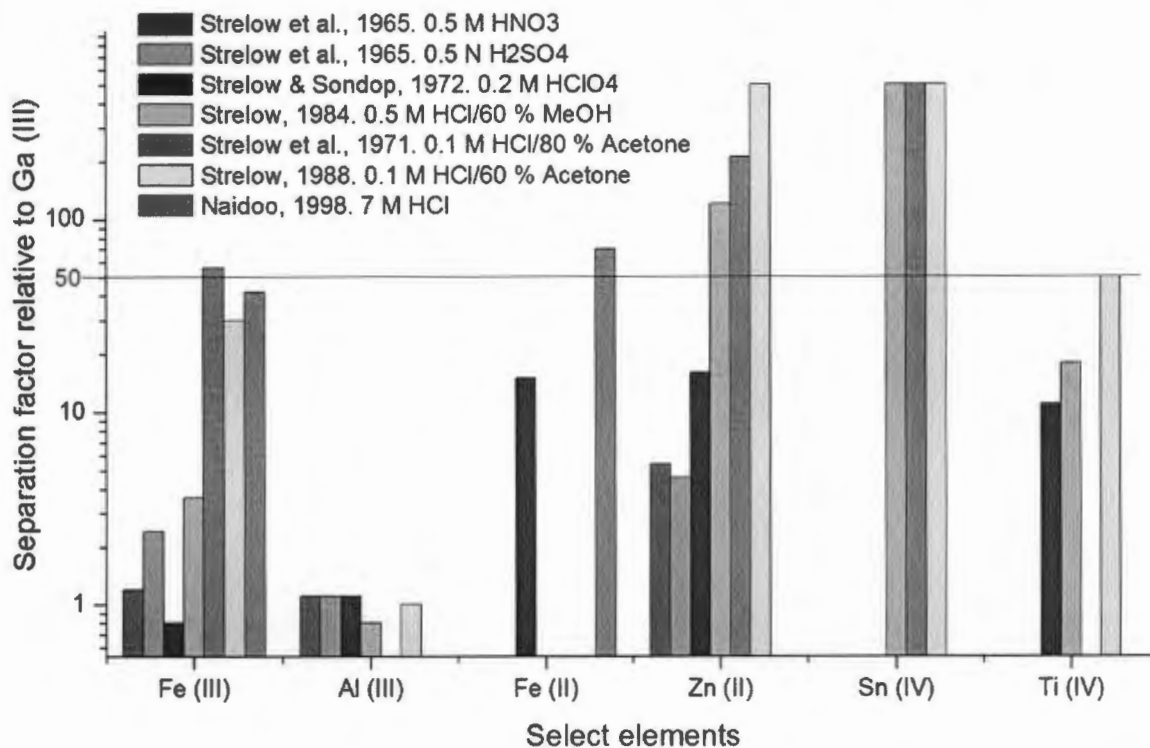


**Figure 2.8: Separation factors of various ions relative to Ga<sup>3+</sup> (from literature)**

Strelow *et al.* (1971) and Strelow (1988) determined distribution coefficients in hydrochloric acid-acetone mixtures (Table 2.5). Both reported high enough separation factors for Zn<sup>2+</sup>, Sn<sup>4+</sup> and Fe<sup>3+</sup> (Figure 2.8, indigo/yellow) but required large columns for separations. Although Strelow *et al.* (1971) did not determine distribution coefficients for Ge<sup>4+</sup>, the authors reported that Ge<sup>4+</sup> could be eluted with 0.1 M HCl. These details are summarised in Table 2.5 below.

**Table 2.5: Overview of distribution coefficients relevant to gallium separations**

Article	Resin	Media	Elements <sup>a</sup>
Strelow <i>et al.</i> , 1965	AG MP50	0.5 N HNO <sub>3</sub> and 0.5 N H <sub>2</sub> SO <sub>4</sub>	Ga, Al, Fe, Zn(II)
Strelow and Sondorp, 1972	AG50W-X8	0.2 M HClO <sub>4</sub>	Ga, Al, Fe, Zn(II), Fe(II), Sn(IV), Ti(IV)
Strelow, 1984	AG MP50	0.5 M HCl/60% MeOH	Ga, Al, Fe, Zn(II), Sn(IV), Ti(IV)
Strelow <i>et al.</i> , 1971	AG50W-X8	0.1 M HCl/80% Acetone	Ga, Fe, Zn(II), Sn(IV)
Strelow, 1988	AG MP50	0.1 M HCl/60% Acetone	Ga, Al, Fe, Zn(II), Sn(IV), Ti(IV)
Naidoo and van der Walt, 2001	Amberchrom CG 71	7 M HCl	Ga, Ge (IV), Zn (II), Fe, Fe (II)

a - elements are +3 oxidation state unless stated otherwise.

The method reported by Strelow *et al.* (1971) has high enough separation factors to separate Fe<sup>3+</sup>, Zn<sup>2+</sup> and Sn<sup>4+</sup> from Ga<sup>3+</sup> with a 0.1 M HCl-80% acetone rinse solution. Ti<sup>4+</sup> is needed to reduce Fe<sup>3+</sup> to Fe<sup>2+</sup>, and Ge<sup>4+</sup> should be easily eluted using 0.1 M HCl (Strelow *et al.*, 1971). No method modification would be needed to remove Al<sup>3+</sup> from alumina-based generators as Ga<sup>3+</sup> can be eluted with 0.5 M HCl-90% acetone while retaining Al<sup>3+</sup>. Van der Meulen and van der Walt (2006) reduced Fe<sup>3+</sup> using either TiCl<sub>3</sub> or SnCl<sub>2</sub> at 60°C in 0.1 M HCl before adding concentrated hydrochloric acid to the aforementioned Fe<sup>3+</sup> containing <sup>67</sup>Ga tracer solution. The solution is passed through a 2.5 ml Amberchrom CG161M column to retain <sup>67</sup>Ga and then elute traces of iron with further rinsing of 6 M HCl and finally eluting the <sup>67</sup>Ga with 0.1 M HCl. The method shows promise by removing more than 99% of impurities but is excluded as it requires elution with 0.1 M HCl.

Subsequently, Naidoo and van der Walt (2001) reported a method of separating <sup>67</sup>Ga from a Ge/Zn target. The method used also removes the majority of Fe<sup>3+</sup> by first reducing iron to Fe<sup>2+</sup> with the addition of Ti<sup>3+</sup>. The method reports a good separation factor for Fe<sup>2+</sup> and a partly adequate separation factor for Fe<sup>3+</sup>. The method also reports a good separation factor of 690 for Ge<sup>4+</sup> and Ga<sup>3+</sup>, satisfying the requirements for a complete separation.

The separation uses an Amberchrom CG 71cd resin column in either high concentration of hydrochloric acid or hydrochloric acid-hydrofluoric acid media. Since  $\text{Ga}^{3+}$  can be eluted with de-ionised water, the eluent satisfies the radiolabelling requirements for PEPT.

Thus, two methods have the potential to be integrated into the radiolabelling method to fabricate tracers with minimal modification. Interestingly, Strelow *et al.* (1971) and Naidoo and van der Walt (2001) both make use of acidic chloride media for the chemical purification of gallium. However, the method developed by Naidoo and van der Walt (2001) is preferable to that of Strelow *et al.* (1971) in that the latter requires a large column as well as large rinsing and elution volumes. Large rinsing and elution volumes increase the time taken to perform the separation and decrease the concentration of the final product.

A recent literature survey indicates that several methods exist to purify the  $^{68}\text{Ga}$  supply. However, the integration of these methods with the current PEPT tracer production method is limited by the medium of the purification solution and the time for purification. The labelling process with  $^{68}\text{Ga}$  on strongly acidic cation exchange resins must be performed in dilute hydrochloric acid, which suggests that the method of Naidoo & van der Walt (2001) could be implemented in tracer production to increase the labelling efficiency of tracers. However, it remains to be established whether this purification can be performed in a short enough time frame to avoid substantial losses of  $^{68}\text{Ga}$  due to radioactive decay.

# Chapter 3

## Experiments

As explained in section 2.6.1, the objective of this study is to extend the lifespan of a 1-year-old  $\text{SnO}_2$   $^{68}\text{Ge}/^{68}\text{Ga}$  generator to produce tracers for PEPT studies consistently. To achieve this objective, the extent of interference of each contaminant with the routine ion exchange resins used at PEPT Cape Town (2.4.4) was first assessed by determining equilibrium distribution coefficients. Next, a separation method to remove the interfering contaminants from Ga was tested before improving the method and, finally, a radiolabelling comparison test was performed to determine the extent of purified Ga. This chapter gives a description of the experimental work performed.

### 3.1 Reagents and equipment

All chemicals were of analytical grade and obtained from Merck Sigma Aldrich as follows: 99.999% fuming stannic chloride was obtained for Sn solutions, with 99.99% anhydrous germanium (IV) chloride in liquid form, crystallised 99.995% titanium (III) chloride, 99.999% anhydrous gallium (III) chloride beads, powered anhydrous 99.999% aluminium (III) chloride and 99.9995% iron chips to be dissolved with hydrochloric acid. 37% ACS grade hydrochloric acid was used for all hydrochloric acid solutions used in this study.

De-ionised water, with a conductivity of greater than  $18 \text{ M}\Omega\cdot\text{cm}^{-1}$ , was obtained from a Millipore MilliQ Reagent Grade Water System. The resins NRW 100 and AG50W-X4 used in these experiments were obtained from Purolite (USA). The resin Amberchrom CG 71 was obtained through Merck Sigma Aldrich GmbH. The 1-year-old 30 mCi  $\text{SnO}_2$   $^{68}\text{Ge}/^{68}\text{Ga}$  generator was purchased from the Radionuclide Production Department at iThemba LABS, Faure, South Africa.

Mechanical shaking for all experiments was performed by a GFL 3015 mechanical shaker. All dilution and solution preparations were performed with a Gilson Pipetman P200N and P1000N. All materials were weighed by a microbalance, model Mettler Toledo classic plus (PB303-S/FACT). All chemical analyses were performed on a Varian 4600 ICP-OES. The Varian 4600 uses an optical emission spectroscopy detector system with a lower detection limit of 100 parts per billion. Radiolabelling experiments were performed with an IKA MS-3 Digital orbital shaker IKA (Figure 3.1).

All radiation measurements were performed with a Capintec CRC-25R ionisation chamber (Figure 3.1). A Watson Marlow 120S/DV peristaltic pump was used for pumping solutions through the resin columns for separation experiments. All the volumetric glassware used was Type A grade manufactured by MBL and Anchor Rand. All plasticware was purchased from Plastpro Scientific.



**Figure 3.1: The IKA MS-3 orbital shaker (left) used for mechanically shaking the vial used for radiolabelling, and the Capintec CRC-25R (right) used for all radioactivity measurements**

## 3.2 Resin and column preparation

### 3.2.1 Resin pre-treatment

The cation exchange resins NRW 100 and AG50W-X4 (Figure 3.2) were used in determining the distribution coefficients of the selected ions present in the generator eluent and in the radiolabelling comparison test. These resins were pre-treated by rinsing with hydrochloric acid to ensure that the resin pH was neutral and that all the counter-ions were in the  $H^+$  form. This pre-treatment removed any possible contaminants in the cation exchange resins, because the large excess of hydrogen ions in the acid displaces the possible cation contaminants bound on the exchange resin. The resins were then rinsed with de-ionised water to remove the excess chloride and hydrogen ions before being dried, to ensure accurate weighing for all experiments.



**Figure 3.2: An AG50W-X series resin**

Approximately 50 grams of each resin were dried at room temperature in a laminar flow hood for at least 72 hours. As the resins have a moderate thermal stability and decompose at temperatures above  $120^{\circ}C$ , gentle heating was utilised to ensure that the resin matrix was not damaged. Removing the residual moisture was required to ensure accurate weighing of the resins and to improve the screening process. The dried resins were screened with a molecular sieve into the standard screen size ranges of  $212-300\ \mu m$  and  $300-600\ \mu m$ , and then placed into 250 ml HDPE bottles filled with 10 ml 37% HCl diluted with 90 ml de-ionised water. These bottles were shaken mechanically for 24 hours and

then left for the resin to settle. The mechanical shaking ensured that the chemical kinetics were sufficient for displacing the contaminants with hydrogen ions. The supernatant was then decanted and replaced with 150 ml de-ionised water. The resin slurry was agitated briefly and left to settle before the supernatant was decanted again. This process was repeated 15 times. The final supernatant was tested for pH neutrality to ensure that the excess acid was washed off. The resins were dried in the same way as they had been previously, in a laminar flow hood, before residual water was removed by further heating on a hot plate at 105°C for 4-8 hours in a glass beaker, until no more moisture could be seen condensing on the beaker wall. Further drying was needed to remove any residual water and to ensure the accurate measurement of mass of each resin.

### **3.2.2 Resin column manufacture**

The columns were made from 2 ml polyethylene syringes, modified by placing 70 µm pore sintered polyethylene frits (SUPELCO Analytical, LOT: 13183-01) at the base of each syringe. The sintered frit ensured that the resin was retained within the syringe column while allowing fluids to pass through. Amberchrom CG-71 resin did not require the same pre-treatment as that of the cation exchange resins. The chromatographic resin was purchased and stored in a 20% ethanol solution, and was rinsed with 7 M HCl to remove the solvent.

The slurry of Amberchrom CG-71 resin and ethanol was poured into each column until the resin settled at the respective volume. A second sintered polyethylene frit was then inserted on top of the resin, followed by a Teflon plug which was fitted with a rubber seal to hold the column together. Three different columns were fabricated from the same size of syringe by varying the column height for final volumes of 2.0, 1.0 and 0.5 ml.

Upon first use of the column, the resins were equilibrated by pumping 7.0 M HCl through the column in a vertical position. By operating the column vertically, any trapped air that could have altered the chemical equilibrium was first removed.

### 3.3 Equilibrium distribution coefficients

Equilibrium distribution coefficient tests were performed for AG50W-X4 and NRW 100 in order to determine the extent of ionic interaction between these resins and the contaminants released by  $\text{SnO}_2$   $^{68}\text{Ge}/^{68}\text{Ga}$  generators. 1.000 g of resin was weighed and added to a 250 ml plastic bottle. 1.00 mmol in 10.0 ml of Fe was added to the bottle containing 1.000 g of resin before the volume was made up to 100.0 ml with 0.005 M HCl. This was repeated with both NRW 100 and AG50W-X4 on each of the selected ions: Fe, Ti, Al, Ga, Sn, Ge and Zn. Ti was included in the study to determine the feasibility of using  $\text{Ti}^{3+}$  as an iron reductant by lowering the iron oxidation state from +3 to +2 with  $\text{Ti}^{3+}$ , the chemical properties of  $\text{Fe}^{3+}$  should differ sufficiently to separate from  $\text{Ga}^{3+}$ . Al was selected to determine if the separation method would be compatible with that of aluminium oxide based  $^{68}\text{Ge}/^{68}\text{Ga}$  generators. The concentration of Ga was selected arbitrarily, as the equivalent concentration of  $^{68}\text{Ga}$  would be below the detection limits of the ICP-OES. Each bottle was shaken for 24 hours, after which the resin slurry was poured into 20 ml separation columns lined with sintered frits used to retain the resin (Figure 3.3, left), while the solution drained into 250 ml volumetric flasks underneath (Figure 3.3, right). The resin was kept submerged while portions of the solution were added incrementally to the separation column. Keeping the resin submerged ensured that the chemical conditions would not alter the chemical equilibrium. The bottle used for shaking was then rinsed with 100.0 ml 0.005 M HCl in 20 ml increments, and decanted into the respective separation columns to remove unbound Ga from the resin surface. The volumetric flasks were made up to 250.0 ml using 0.005 M HCl before being mixed thoroughly. 20 ml of each volumetric flask were then decanted into 20 ml sample vials before being analysed by ICP-OES.

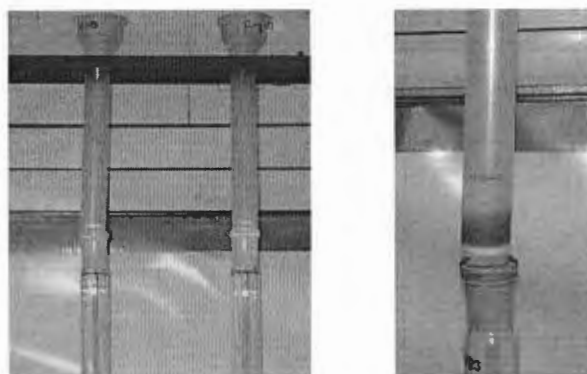


**Figure 3.3: Layout of the separating column above the volumetric flask (left), and a close up of the separating column retaining resin while the solution drains off (right)**

### **3.4 Separation method**

The method was first tested by performing chemical separations for Zn, Al, Fe, Sn and Ge against Ga. The test was repeated to determine how well all the above elements separate from Ga on a single column before modifying the method to reduce the required chemicals and process time.

#### **3.4.1 Elution profiles**

After confirming the presence and interference of the contaminants, chemical separations were performed on Amberchrom CG 71 to separate Ga from the contaminants Zn, Al, Fe, Sn and Ge. Experiments were performed for each respective contaminant with Ga. Five 2 ml columns (9 mm Ø x 35 mm) were made up as described in the column preparation method (section 3.2.2). Elution profiles were then plotted to determine the effective volumes used in the method to separate each contaminant from Ga.

The columns were equilibrated with 15 ml 7.0 M HCl before each column was loaded with 7 ml loading solution. The loading solution is made up of 2 ppm Ga and 2 ppm of the contaminant in 7.0 M HCl. Loading solutions were produced for the contaminants Fe, Zn, Sn, Ge and Al. The concentration of 2 ppm was selected based on the quantified contaminant concentrations from literature (De Blois *et al.*, 2011). Solutions were

pumped through the columns at  $\pm 2.5$  ml/min using a peristaltic pump, while the eluent was collected in aliquots. The eluents were collected in increments in order to determine the minimal volume of each solution for elution. The columns were rinsed with a 15 ml 7.0 M HCl rinse solution in 5 ml increments. The column was then left to pump dry before rinsing the tubing with distilled water. Caution was taken not to expose the column to any distilled water as this would remove the gallium prematurely. Finally, the gallium was eluted by passing 5 ml distilled in the opposite direction that gallium was loaded on, and the eluent was collected for analysis.

### **3.4.2 Column separation**

A synthetic column separation test was developed based on the results obtained from the elution profiles. It was difficult to control the concentration of  $^{68}\text{Ga}$  due to its rapid decay and, therefore, stable ions were first used to create a synthetic generator eluent. Furthermore, this test took into account any possible synergistic ionic effects, and reduced the amount of excess reagents and resin used. The 37% hydrochloric acid used in subsequent experiments was passed through a 5.0 ml Amberchrom CG 71 column in aliquots of 100 ml using a peristaltic pump at a flow rate of 2.0 ml/min in order to further remove residual iron from the system. The column was regenerated by passing 20 ml of de-ionised water in between aliquots to avoid saturating the column.

A 2 ml Amberchrom CG 71 resin column was prepared and equilibrated in the same way as described previously. A loading solution of 3.0 ml of 2 ppm Zn, Sn, Ga and Ge solution in 0.6 M HCl was then made up to 7.0 M HCl with concentrated HCl. The loading solution was pumped through the column and the eluent was collected for analysis. 15.0 ml of 7.0 M HCl rinse solution was then passed through the column at 2.5 ml/min and the eluent was collected in 5.0 ml increments for analysis using an ICP-OES. Finally, the Ga was eluted with 10.0 ml distilled water at a rate of 2.5 ml/min and the eluent was collected in 5 ml increments for analysis.

### 3.4.3 Method to determine column size

The column separation test determined the reduced volumes for the rinse and elution steps of the method. The synthetic generator eluent was adjusted successfully to 7 M HCl, as gallium had been successfully retained by the resin. This confirmed the compatibility of the method with the eluent from an aged  $\text{SnO}_2$   $^{68}\text{Ge}/^{68}\text{Ga}$  generator.

Three resin columns with volumes 2.0, 1.0 and 0.5 ml were prepared as described in Section 3.2. A  $\text{SnO}_2$   $^{68}\text{Ge}/^{68}\text{Ga}$  generator was eluted with 4.5 ml of 0.6 M HCl, the first millilitre of which was discarded. An eluent sample containing 1 mCi of  $^{68}\text{Ga}$  in approximately 150-200  $\mu\text{L}$  0.6 M HCl was added to a loading solution of 3.0 ml of 2 ppm Zn, Sn, Ga and a Ge solution in 0.6 M HCl. The loading solutions were then made up to 7 M HCl with concentrated HCl (37%). The columns were equilibrated with at least seven times the volume of each column before the loading solutions were passed through the respective columns.

For the 2.0 ml column, a rinse volume of 5 ml 7.0 M HCl was used and collected before the column was left to run dry. 4.0 ml of de-ionised water was used and collected in 1 ml increments to elute the purified  $^{68}\text{Ga}$  off the column. For the 1.0 and 0.5 ml columns, rinse volumes of 2.5 ml and 2.0 ml 7.0 M HCl, respectively, were used and collected, before the columns were left to run dry. 2.0 ml of de-ionised water was used and collected in 0.5 ml increments to elute the purified  $^{68}\text{Ga}$  off the column.

### 3.5 Tracer labelling comparison test

Both the purified and un-purified generator eluents were used to radiolabel NRW 100 and AG50W-X4 resins with  $^{68}\text{Ga}$ . This test was designed to illustrate whether the purification method would lead to an improvement in radiolabelling efficiency, and the potential application in fabricating tracer particles for PEPT studies. The standard radiolabelling procedure was performed in triplicate, with two resin beads used in each case. A second set of radiolabelling experiments was then performed using the eluent purification method, followed by the same evaporation and shaking steps as those used in the standard radiolabelling method.

# Chapter 4

## Results and Discussion

As the  $^{68}\text{Ge}/^{68}\text{Ga}$  generator ages over the 6-9 months of its lifespan, both the increase in the amount of contaminant and the decay of supply radionuclide,  $^{68}\text{Ge}$ , reduce the performance of the radiolabelling process.

Section 4.1 indicates the equilibrium distribution coefficient values for gallium, germanium, iron, tin, zinc, titanium and aluminium ions used to determine the degree of selectivity of NRW100 and AG50W-X4 for each element. Section 4.2 reports on the performance of the separation method selected. The data from a 2 ml Amberchrom CG71 column to separate gallium from each of the selected contaminants germanium, aluminium, iron, tin and zinc is described before a report on multiple separations of all the ions from gallium on a single column is given. This section concludes with the results of the different column sizes tested. A custom-built separation panel to improve the separation method is described in detail in section 3.5. Section 4.4 reports on the results of a comparison test performed to determine the effect of  $^{68}\text{Ga}$  purity on the radiolabelling method.

## 4.1 Equilibrium distribution coefficients, $K_d$

Equilibrium distribution coefficients were determined, by the method described in Section 3.4, to investigate the extent of competition between Fe, Al, Ti, Zn, Sn, Ge and  $\text{Ga}^{3+}$  for exchange with  $\text{H}^+$  ions on NRW 100 and AG50W-X4. Tests were performed to indicate an order of affinity of each contaminant ion under the standard radiolabelling conditions, as the equilibrium distribution coefficient  $K_d$  is a useful measure of the ability of an ion exchange resin to remove a specific ion from a solution. The standard radiolabelling conditions were determined by van Heerden (2012) to be approximately 500  $\mu\text{L}$  of 0.005 M HCl.

The equilibrium distribution coefficients for the cation exchange resins AG50W-X4 and NRW 100 were then calculated from the results obtained from the test described in Section 3.4 and reported in Table 4.1. Ionic species that had precipitated under the standard radiolabelling conditions were labelled as “ppt” (precipitated) as the solid material would be unlikely to be sorbed on the selected resins. Ionic species with  $K_d$  values that had been calculated to be greater than 10000 were deemed to be highly selective for NRW 100 and AG50W-X4, and, as such listed as  $>10^5$ .

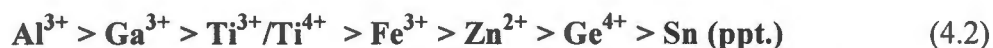
**Table 4.1: Equilibrium distribution coefficients of AG50W-X4 and NRW 100**

Element	Cation Exchange Resin	
	AG50W-X4	NRW100
Ga (III)	$>10^5$	$>10^5$
Fe (III)	1910	2530
Al (III)	$>10^5$	$>10^5$
Ti	2350	5800
Zn (II)	1630	2740
Sn (IV)	ppt.	ppt.
Ge (IV)	1379	1447

After calculating the distribution coefficient of each ionic species on NRW 100, a simplified elution order was predicted and is reported as:



Again, a simplified elution order is predicted for the same ionic species on AG50W-X4:



Comparing these elution orders, both resins showed similar affinities for the above-listed ions, with the exception of  $\text{Fe}^{3+}$  and  $\text{Zn}^{2+}$ . NRW 100 had a greater affinity with  $\text{Zn}^{2+}$  over  $\text{Fe}^{3+}$ , whereas AG50W-X-4 had a greater affinity with  $\text{Fe}^{3+}$  over  $\text{Zn}^{2+}$ .

The ion  $\text{Al}^{3+}$  is not a contaminant found in  $\text{SnO}_2$  column-based  $^{68}\text{Ge}/^{68}\text{Ga}$  generators, but was investigated in this study to determine compatibility with alumina column-based  $^{68}\text{Ge}/^{68}\text{Ga}$  generators. Both resins NRW 100 and AG50W-X4 showed a greater affinity with  $\text{Al}^{3+}$  over  $\text{Ga}^{3+}$  (Equation 4.1 and 4.2), which indicates that  $\text{Al}_2\text{O}_3$  column-based  $^{68}\text{Ge}/^{68}\text{Ga}$  generators would encounter greater competition between contaminants and gallium during the radiolabelling process. Solutions of  $^{68}\text{Ga}$  that are contaminated with aluminium should be purified before proceeding with the standard radiolabelling procedure.

The ions  $\text{Ti}^{3+/4+}$  were investigated as a potential oxidising agent to remove the contaminant  $\text{Fe}^{3+}$ , which shares similar chemical behaviour with  $\text{Ga}^{3+}$  and would thus compete for uptake on a cation exchange resin. By reducing  $\text{Fe}^{3+}$  to  $\text{Fe}^{2+}$ , the lower valence  $\text{Fe}^{2+}$  should have a lower affinity.  $\text{Fe}^{3+}$  is assumed to be the result of environmental contamination and can be expected to vary in concentration with daily tracer production. Therefore  $\text{Ti}^{3+/4+}$  should be added in excess to ensure that the bulk of  $\text{Fe}^{3+}$  is reduced. Equations 4.1 and 4.2 show that NRW 100 and AG50W-X4 have a lower affinity for  $\text{Fe}^{3+}$  than  $\text{Ti}^{3+/4+}$ , therefore any excess  $\text{Ti}^{3+/4+}$  would be sorbed more effectively by the resin than  $\text{Fe}^{3+}$ . As the presence of  $\text{Fe}^{3+}$  would be less likely to interfere with  $\text{Ga}^{3+}$  than it would with  $\text{Ti}^{3+/4+}$ , an alternative method was investigated to remove  $\text{Fe}^{3+}$  without adding  $\text{Ti}^{3+/4+}$ .

A preventive approach was taken by removing trace quantities of  $\text{Fe}^{3+}$  from the supply of concentrated hydrochloric acid, and fabricating an enclosed panel for the entire separation process, which limited further exposure of  $^{68}\text{Ga}$  to the environment (Figure 4.6).

Under ambient conditions, cations with a higher valence are typically preferred by strong cation exchange resins. Although  $\text{Fe}^{3+}$  has a greater valence than  $\text{Zn}^{2+}$ , Equation 4.1 shows that, for equal concentrations of both ions, NRW 100 has slightly greater selectivity for  $\text{Zn}^{2+}$ . This has important implications for the ion exchange process, as the concentration of zinc increases constantly due to the decay series (Equation 2.6) of  $^{68}\text{Ga}$  to stable zinc.  $^{68}\text{Ge}$  decays to  $^{68}\text{Ga}$ , while  $^{68}\text{Ga}$  decays simultaneously to stable zinc, resulting in a decay equilibrium once both  $^{68}\text{Ge}$  and  $^{68}\text{Ga}$  decay at equal rates. Once the  $^{68}\text{Ge}/^{68}\text{Ga}$  generator is under decay equilibrium, the amount of zinc produced exceeds the amount of  $^{68}\text{Ga}$  present, as stable zinc does not decay. This potential for increased concentration of zinc ions could lead to an increase in both the amount of zinc that is sorbed by the resin and the competition for a limited number of available exchange sites. An increase in ionic concentration of a less selective ion would increase the amount of that ion sorbed by the resin. Despite zinc having a lower affinity for NRW100 than it has for gallium, as shown in Equation 4.1, the higher concentrations of zinc encountered in routine  $^{68}\text{Ge}/^{68}\text{Ga}$  generator elutions could reduce the labelling of  $\text{Ga}^{3+}$ , and should be removed from the solution before radiolabelling. Although AG50W-X4 has a greater affinity for  $\text{Fe}^{3+}$  than it has for  $\text{Zn}^{2+}$ , as shown in Equation 4.2, the presence of zinc could still reduce  $\text{Ga}^{3+}$  labelling in the same mode as that described for NRW100. By removing competing ions, availability for the limited number of exchange sites could improve the radiolabelling performance of  $^{68}\text{Ga}$ .

As shown in Table 4.1, the contaminant ion  $\text{Ge}^{4+}$  showed the lowest values of  $K_d$  of all the ions under study for both NRW 100 and AG50W-X4, suggesting that it would have the lowest sorption on NRW 100 and AG50W-X4 for the selected ions. In practice, the concentration of  $^{68}\text{Ge}$  contained in the generator eluent is likely to be lower than that of the other contaminants; however, even small amounts of  $^{68}\text{Ge}$  contamination pose a radiation hazard due to the lengthy half-life of  $^{68}\text{Ge}$  ( $t_{1/2} = 280$  days). The risk involved in contamination for PEPT studies supports the principle of implementing a purification method to remove  $^{68}\text{Ge}$  from the  $^{68}\text{Ga}$  eluent.

No  $K_d$  value was determined for  $\text{Sn}^{4+}$ , since  $\text{Sn}^{4+}$  proved to be unstable in the radiolabelling conditions and precipitated in dilute hydrochloric acid. The solution formed opaque, white and gelatinous sediment in both the NRW 100 and AG50W-X4 shaking bottles, suggesting that  $\text{Sn}^{4+}$  would not compete for the limited amount of exchange sites.

## 4.2 Separation method

### 4.2.1 Elution profiles

Column separations of the contaminants  $\text{Al}^{3+}$ ,  $\text{Fe}^{3+}$ ,  $\text{Zn}^{2+}$ ,  $\text{Ge}^{4+}$  and  $\text{Sn}^{4+}$  were performed on an Amberchrom CG71 chromatographic column in 7.0 M hydrochloric acid. Contaminants were tested individually against  $\text{Ga}^{3+}$  to determine the extent to which they are separated from the target ion. In every test, each contaminant ion and  $\text{Ga}^{3+}$  was first loaded onto the column, and then rinsed off with small incremental volumes of elution solution. In this section, the elution profiles of each experiment are plotted as mass versus total volume of solution used.

Figure 4.1 shows the elution profile for  $\text{Al}^{3+}$  and  $\text{Ga}^{3+}$ , which were loaded onto the column in a solution of 7.0 M HCl. The bulk of aluminium was eluted before the rinse step. Although both ions share the same valence, the high HCl concentration yields the  $\text{GaCl}_6^{3-}$  specie, which is assumed to interact with the chromatographic resin more than does the aluminium chloride specie. In the rinse step, residual amounts of  $\text{Al}^{3+}$  are further removed from the column. The rinse volume of approximately 15 ml could be increased further to remove the remaining  $\text{Al}^{3+}$ , as approximately 4% of the total recovered Al was found in the final product eluate.

No  $\text{Ga}^{3+}$  had been lost during the load or rinse step, 97% of the total having been recovered in the first 5 ml of de-ionised water. Therefore this method indicates potential to remove all the  $\text{Al}^{3+}$  from  $\text{Ga}^{3+}$ .

The separation of  $\text{Ga}^{3+}$  and  $\text{Fe}^{3+}$  is difficult due to the similar chemical properties of the ions (Table 2.4), as well as the varying amount of  $\text{Fe}^{3+}$  eluted from the generator with

fluctuations in environmental contamination. The inability to separate the two ions is supported by the column separation (Figure 4.2) between  $\text{Fe}^{3+}$  and  $\text{Ga}^{3+}$ , with all the  $\text{Fe}^{3+}$  being eluted with  $\text{Ga}^{3+}$  from the column. Finally, all the  $\text{Fe}^{3+}$  had been eluted within the first 5 ml of de-ionised water passed through the column. Despite using analytical grade chemicals and high purity water, a significantly larger amount of  $\text{Fe}^{3+}$  was recovered than had been added to the initial load solution, with approximately 200% the environmental contaminant recovered. The excessive recovery of  $\text{Fe}^{3+}$  is assumed to be the result of further environmental contamination, which reinforces the need to seal the separation process from the environment.

In the  $\text{Fe}^{3+}/\text{Ga}^{3+}$  elution, all the  $\text{Ga}^{3+}$  recovered was eluted in the first 5 ml of de-ionised water in combination with  $\text{Fe}^{3+}$ , which can be regarded as an unsuccessful separation. The short half-life of  $^{68}\text{Ga}$  requires that the separation method be temporally efficient and simplistic to avoid loss of  $^{68}\text{Ga}$  due to radioactive decay. This highlights the importance of taking additional steps to avoid environmental contamination with  $\text{Fe}^{3+}$ , such as removing it from the chemicals used beforehand, as well as the construction of an enclosed separation panel.

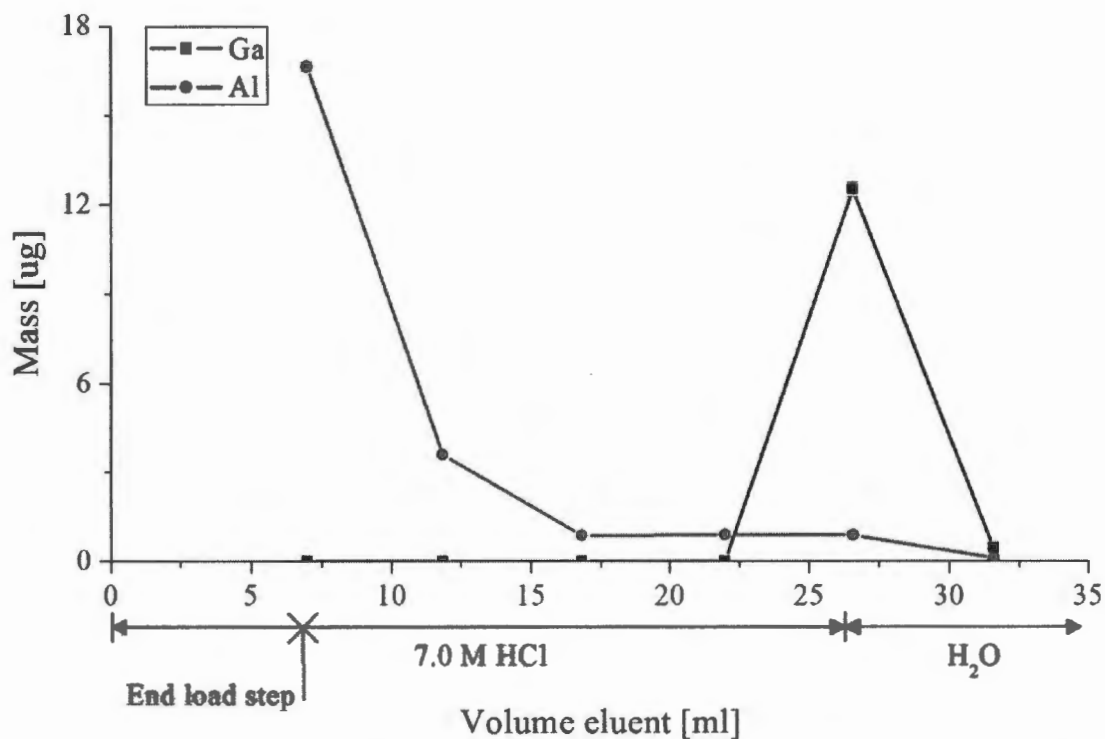


**Figure 4.1: Elution profile of Al<sup>3+</sup>/Ga<sup>3+</sup> in 7 M HCl on a 2 ml Amberchrom CG71 column, followed by Ga<sup>3+</sup> elution step using de-ionised water**

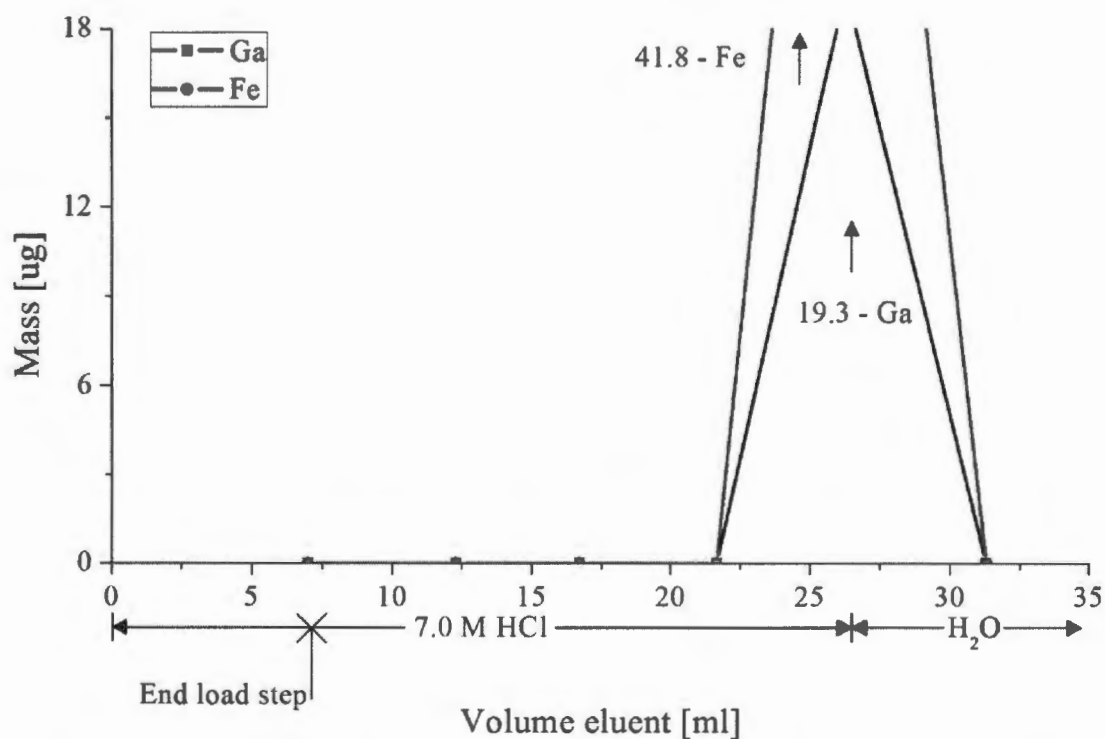


**Figure 4.2: Elution profile of Fe<sup>3+</sup>/Ga<sup>3+</sup> in 7 M HCl on a 2 ml Amberchrom CG71 column, followed by Ga<sup>3+</sup> elution using de-ionised water**

The separation by elution of  $\text{Zn}^{2+}$  from  $\text{Ga}^{3+}$  performed the most efficiently of all the contaminants tested, as shown in Figure 4.3, in terms of requiring the least volume of solution to elute. Approximately 75% of the total  $\text{Zn}^{2+}$  recovered was eluted in the column-loading stage, and the remaining  $\text{Zn}^{2+}$  was removed within the first 5 ml of the rinse stage. The  $\text{Zn}^{2+}/\text{Ga}^{3+}$  separation could have been optimised further by using a smaller rinsing volume, which, in turn, would have reduced the time taken to perform each separation and the loss of  $^{68}\text{Ga}$  due to radioactive decay.  $\text{Ga}^{3+}$  was eluted readily within the first 5 ml of de-ionised water.

The separation of  $\text{Ge}^{4+}$  from  $\text{Ga}^{3+}$  proved unsuccessful, as seen in Figure 4.4, as neither  $\text{Ge}^{4+}$  nor  $\text{Ga}^{3+}$  had been eluted off the column in the load or rinse step, and the total masses of both ions recovered in the first increment of de-ionised water. This outcome is not in accordance with that anticipated from literature, nor the values of distribution coefficients as described in Section 2.5.3. By comparison, this study reports distribution coefficients of  $>10^5$  for  $\text{Ga}^{3+}$  and 1447 for  $\text{Ge}^{4+}$  in different concentrations of hydrochloric acid. Despite a large difference in distribution coefficients, this should have led to a successful separation in both media, and it is unclear why the  $\text{Ga}^{3+}$  and  $\text{Ge}^{4+}$  did not separate as expected. The method described by Naidoo (1998) used a larger column in varying mixtures of hydrofluoric-hydrochloric acid, attempting to separate much larger quantities. A larger column requires a larger rinse volume. Therefore, the two ions could possibly be separated by increasing the rinse volume or further reducing the column size.

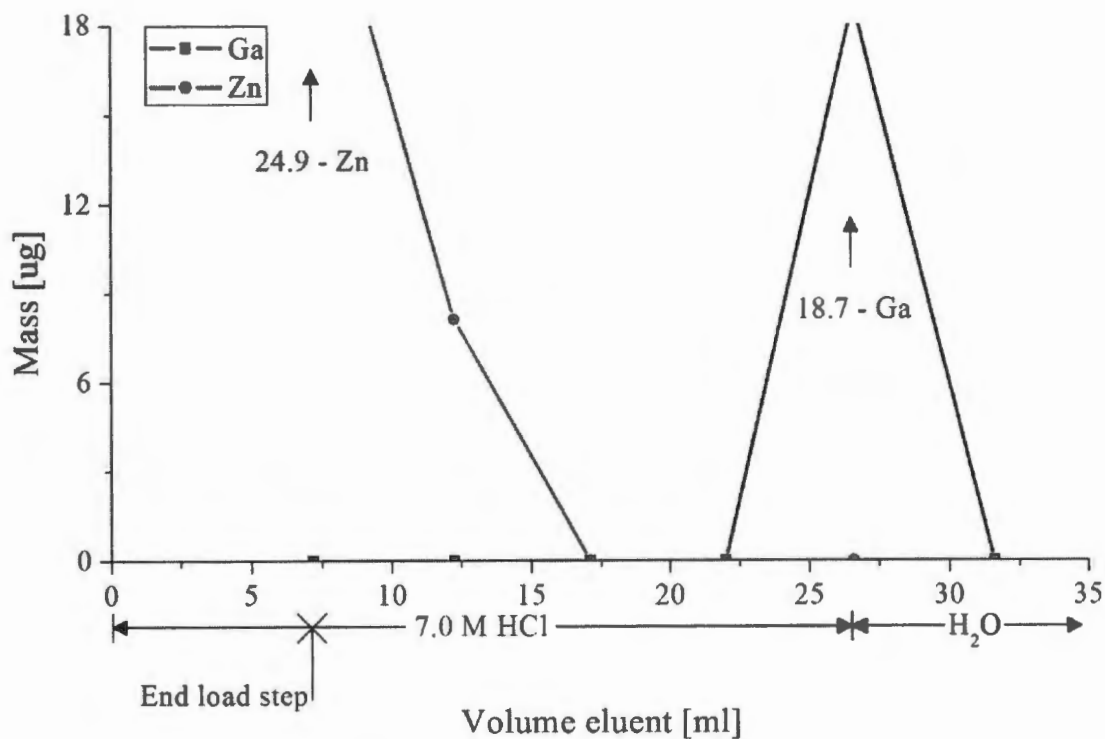


**Figure 4.3: Elution profile of Zn<sup>2+</sup>/Ga<sup>3+</sup> in 7 M HCl on a 2 ml Amberchrom CG71 column, followed by Ga<sup>3+</sup> elution using de-ionised water**

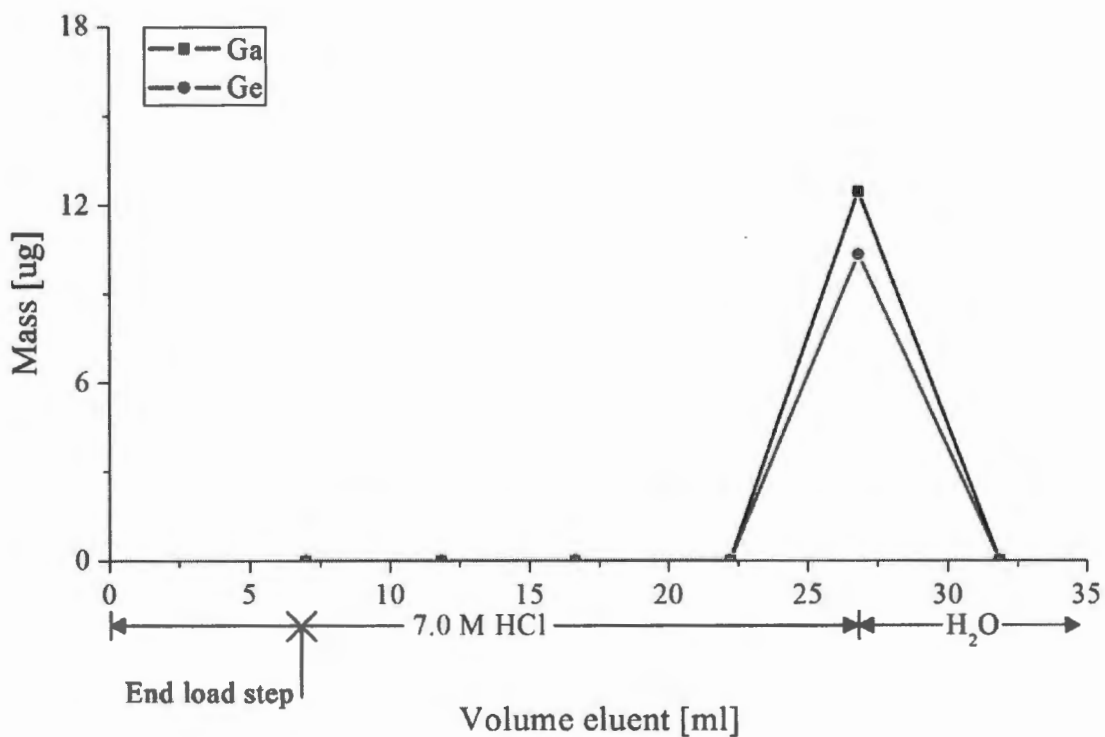


**Figure 4.4: Elution profile of Ge<sup>4+</sup>/Ga<sup>3+</sup> in 7 M HCl on a 2 ml Amberchrom CG71 column, followed by Ga<sup>3+</sup> elution using de-ionised water**

The ion  $\text{Sn}^{4+}$  was shown to be responsible for a gelatinous precipitate when performing equilibrium distribution coefficients under radiolabelling conditions. The separation of  $\text{Ga}^{3+}$  from  $\text{Sn}^{4+}$  was included in the study, to investigate whether  $\text{Sn}^{4+}$  is present in the radiolabelling process. Less than  $1.0 \mu\text{g}$  of  $\text{Sn}^{4+}$  was recovered from the initial load step (Figure 4.5), and no  $\text{Sn}^{4+}$  was recovered in the rinse step. There was also no  $\text{Ga}^{3+}$  recovered in the load or rinse step. Less than  $1 \mu\text{g}$  of  $\text{Sn}^{4+}$  was recovered along with all the  $\text{Ga}^{3+}$  recovered within the first 5 ml of de-ionised water.

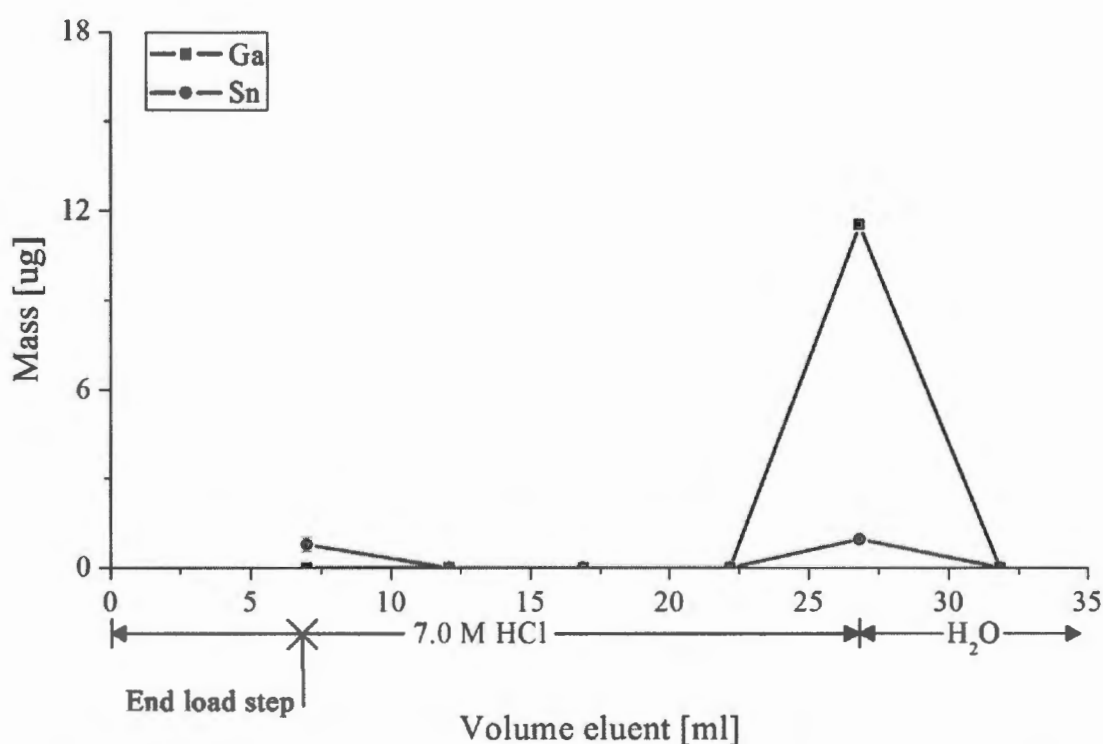


**Figure 4.5: Elution profile of  $\text{Sn}^{4+}/\text{Ga}^{3+}$  in 7 M HCl on a 2 ml Amberchrom CG71 column, followed by  $\text{Ga}^{3+}$  elution using de-ionised water**

In summary, using a 2 ml Amberchrom CG71 column in 7 M hydrochloric acid,  $\text{Al}^{3+}$  and  $\text{Zn}^{2+}$  were readily separated from  $\text{Ga}^{3+}$ .  $\text{Sn}^{4+}$  was partially separated from  $\text{Ga}^{3+}$ , whereas neither  $\text{Fe}^{3+}$  nor  $\text{Ge}^{4+}$  was separated at all. The possibility of some oxidation/reduction occurring when all the selected ions are mixed together is not ruled out, and so the method was tested further with all the ions in solution.

### 4.2.2 Modified separation method

The process of the new separation method (Figure 4.6) is listed below, designed to be integrated into the standard radiolabelling procedure. Firstly, the generator is eluted to obtain 3.5 ml of  $^{68}\text{Ga}$  in 0.6 M HCl, the same as that for the standard radiolabelling procedure. 4.0 ml of concentrated HCl is drawn into a 5 ml syringe (2) mounted above the storage bottle (3) before being decanted into a loading vial (Figure 4.6, 1). The load solution is pumped through the column, in an upwards direction via the green tap (8), through the tubing and red/white tap (10), then down and out through the red tap (9) towards the waste beaker. As the loading vial is emptied, the grey tap (6) is opened toward the column to allow the 7.0 M HCl to rinse the column. After at least 2 ml has passed through the column, the grey tap is closed again and the column left to pump dry for approximately 1 minute.

The pump is stopped and the column closed off by rotating the green and red/white tap downwards. The blue tap (5) is opened toward the column and the de-ionised water is displaced through negative pressure by pulling the 5 ml syringe (11) upwards. Residual HCl is removed from the tubing and taps by filling the syringe with de-ionised water before discarding the rinse water through the red tap. The syringe is then filled again with the required elution volume. The red tap is then closed downwards before the red/white tap is turned upwards. Afterwards, the green and yellow (8) taps are turned towards each other. The de-ionised water in the syringe (11) is pushed slowly through the column in the reverse direction of conventional flow, and out via the yellow tap into a vial (12), to be transported for the evaporation step in the standard radiolabelling procedure.

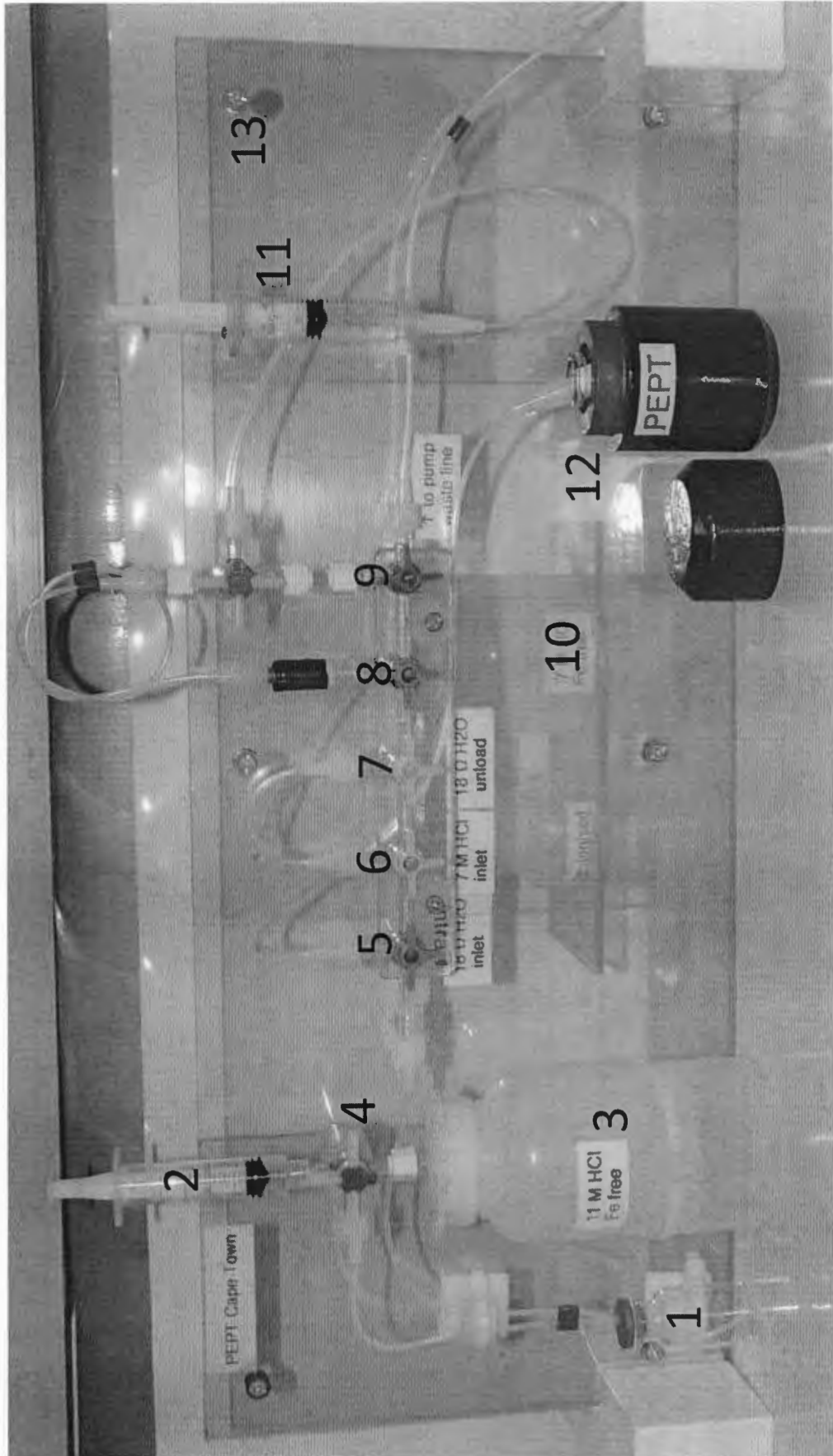


Figure 4.6: Layout of radiolabelling method

### 4.2.3 Column separation

A 2 ml Amberchrom CG71 column was prepared, as described previously, and the acid medium was purified to remove traces of iron. The separation panel was used for this set of experiments, to reduce the level of potential contamination with iron. As the concentration of ions eluted from the generator varies daily, each synthetic separation was performed using slightly varying volumes, the intention being that any fluctuations would correspond to fluctuations in the performance of the radioactive separations. Five separations were performed in total.

The results of the first separation (Figure 4.7) did not agree with the results of the individual column separations for iron and gallium. Zinc was the only ion eluted during the load step as the lower valence ion is assumed to be retained less by the resin. During the rinse step, the remainder of the zinc was eluted within the first incremental volume of solution. Approximately 1.0  $\mu\text{g}$  of  $\text{Ga}^{3+}$  was eluted off the column in the second rinse aliquot, along with 17  $\mu\text{g}$  of iron. A potential explanation for the large amount of eluted iron is that the iron was reduced to a lower valence, thus enabling its removal. The extent of the iron contamination was made evident at this point, as the solutions had all been pre-treated to remove iron. No ions were passed through the column during the final rinse aliquot. After running the column dry, the  $\text{Ga}^{3+}$  was eluted using 10 ml of de-ionised water in two increments. Iron, germanium and gallium were found in the first increment only, with roughly equal mass portions. The separation of germanium behaved similarly to that in the individual contaminant column separation; in disagreement, again, with the results reported by Naidoo (1998).

After rinsing and equilibrating the column, it was loaded again with the synthetic generator eluent, and the load solution was collected for analysis. Zinc was again eluted in the load step, with no other ions detected (Figure 4.8). From the initial rinse aliquot, the remainder of the zinc was eluted, along with a small amount of tin. No other element was detected in the second and third rinse increments. Gallium, germanium and iron were again collected in the first increment of de-ionised water, with a slightly smaller amount of iron, as compared with that of the first separation.

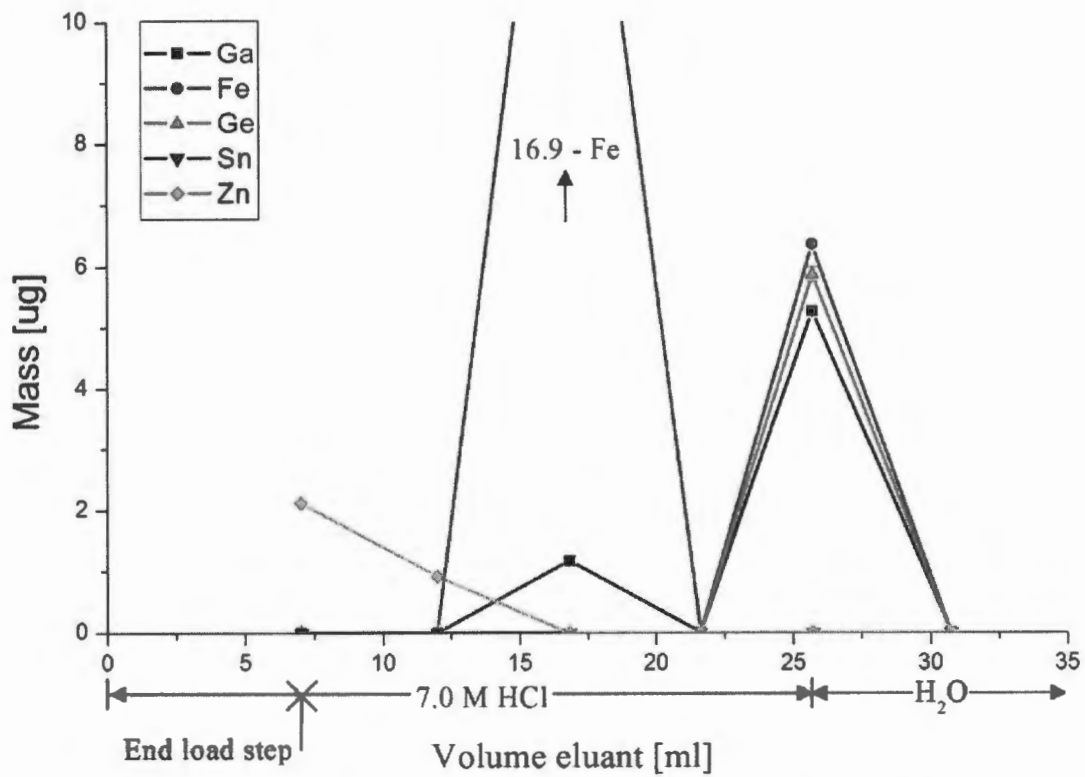


**Figure 4.7: First of five column separations of ions on a 2 ml Amberchrom CG71 column**

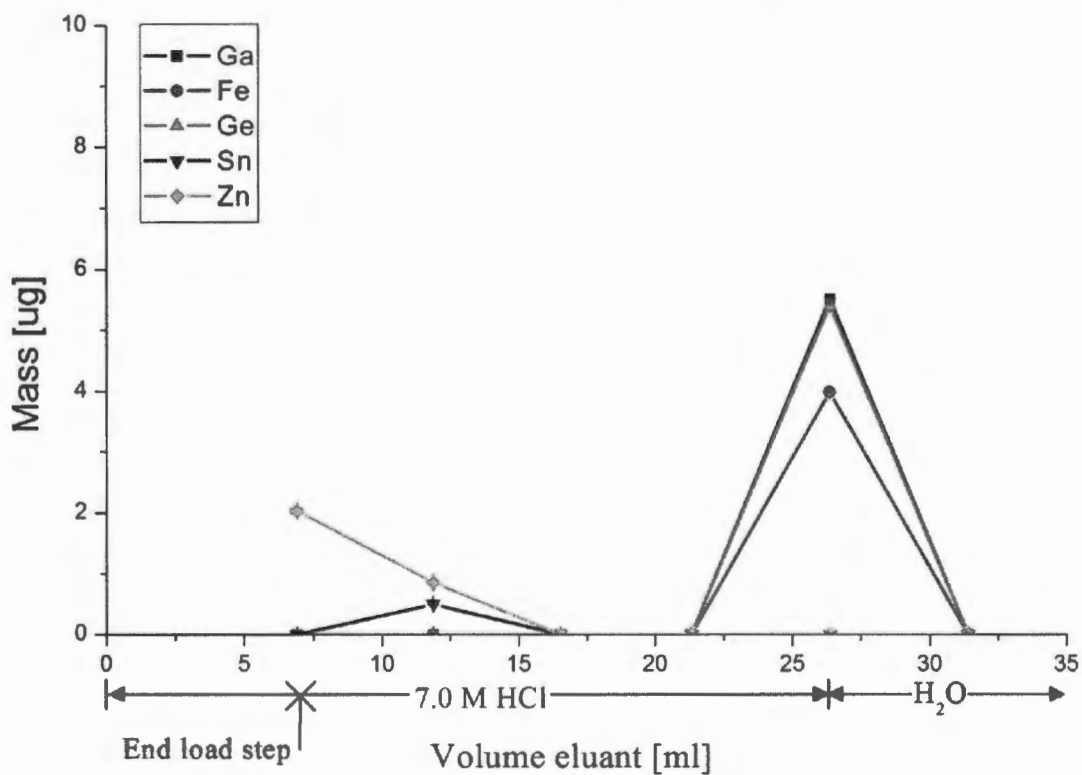


**Figure 4.8: Second of five column separations of ions on a 2 ml Amberchrom CG71 column**

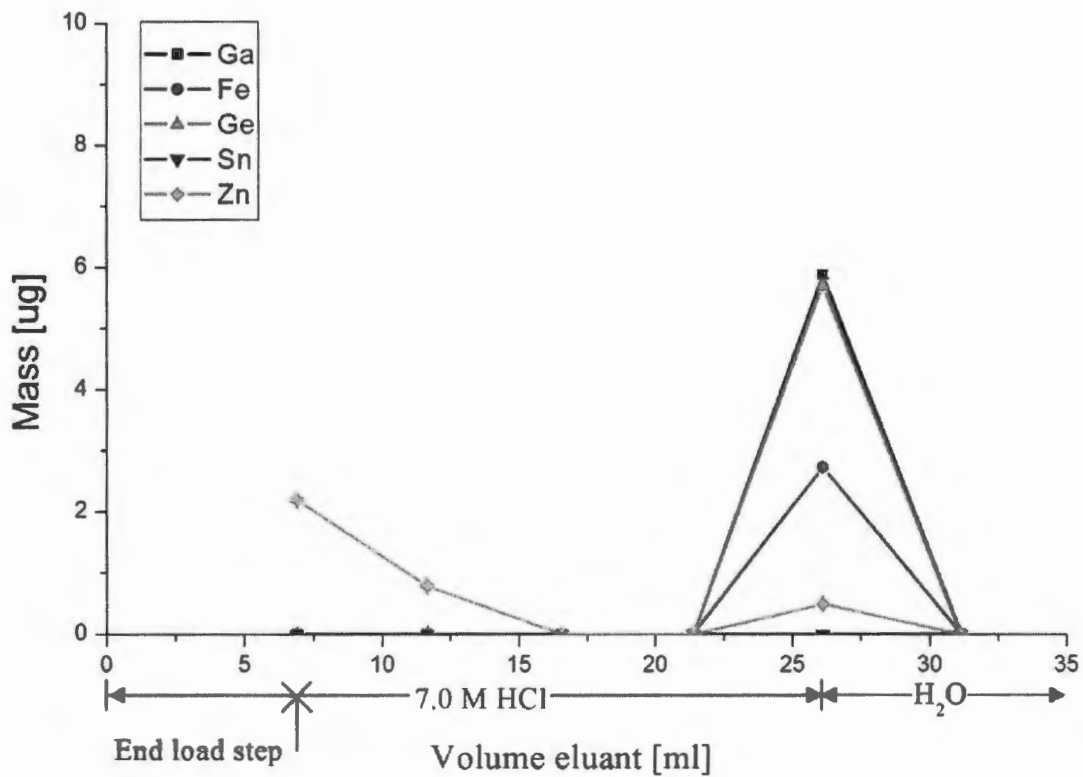
A higher purity and relative yield of gallium was achieved in the second separation in comparison with that of the first separation. The variation in separation can be attributed to the difference in ion concentrations between different separation tests.

In the third column separation, the load step yielded a similar result to that of the first two separations, where only zinc was eluted (Figure 4.9). Zinc was eluted again in the first increment of the rinse step, with no further elements detected in the second and third increments. Unexpectedly, a small amount of zinc was eluted within the first increment of de-ionised water. With a similar outcome to those of the first and second separations, gallium, germanium and iron were eluted in the first increment. The third column separation had a smaller amount of iron and the presence of approximately 0.5 µg of zinc. The reason for zinc being recovered in the de-ionised water eluate is unknown.

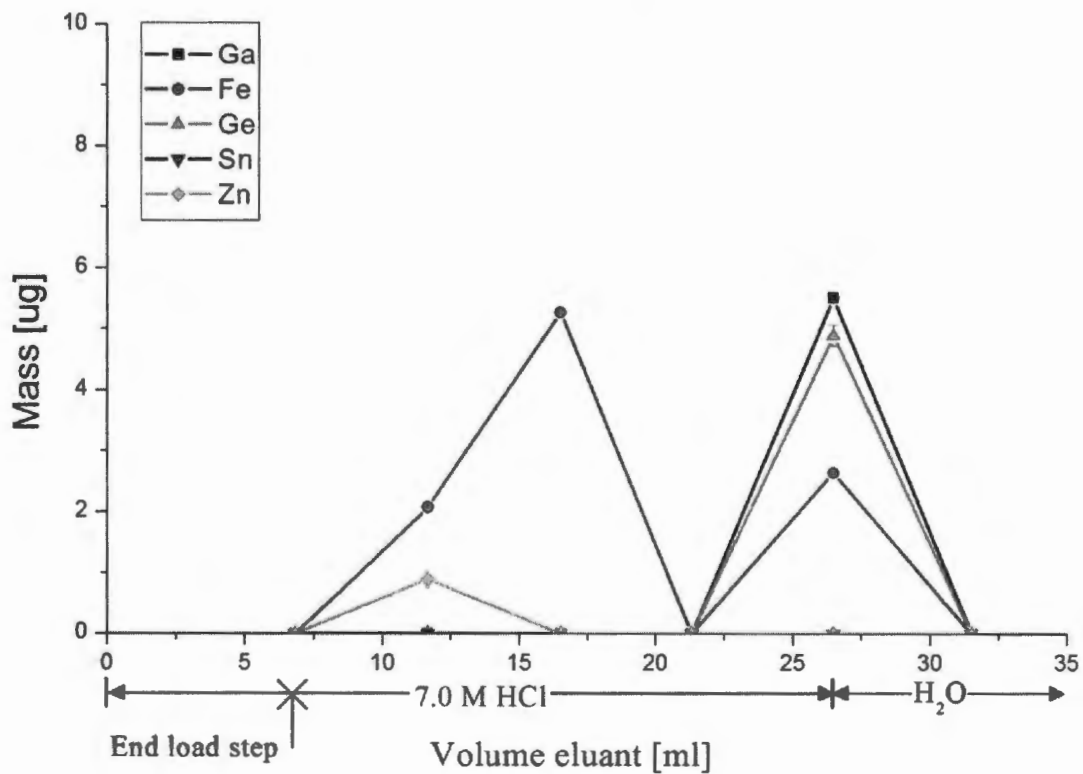
Despite the presence of zinc in the final solution, the purity of gallium from the third separation was assumed to be more suited to radiolabelling, as less of the iron had been recovered. Iron needs to be removed from the radiolabelling process as it is expected to compete with  $^{68}\text{Ga}$  for uptake on the resin (Table 4.1).

Figure 4.10 shows none of the elements being eluted in the initial load step of the fourth separation. Despite no zinc being eluted in the load step, the remainder of the recovered zinc was collected in the first aliquot of the rinse step, along with 2.0 µg of iron. The next increment yielded a further 5.2 µg of iron. The behaviour of iron in the fourth separation is similar to that of the first separation. The same cause is suspected for the elution of iron in the rinse step, with the reduction of the element to a lower valence.

No further elements having been detected in the final rinse increment, the column was pumped dry. The first aliquot in the rinse step recovered gallium, germanium and iron, which was relatively similar to the second and third column separation. The gallium product was of slightly higher purity than that of the third column separation, with similar yields in gallium, germanium and iron, as well as no detectable zinc.



**Figure 4.9: Third of five column separations of ions on a 2 ml Amberchrom CG71 column**



**Figure 4.10: Fourth of five column separations of ions on a 2 ml Amberchrom CG71 column**

A final separation with the same column was performed to confirm the reproducibility of the method, and to determine whether the column performance degrades with repeated use (Figure 4.11). The bulk of zinc recovered was eluted off the column in the load step, as expected. The remaining zinc was eluted in the first increment of the rinse step. No further elements were eluted in the remainder of the rinse step.

The first aliquot of de-ionised water eluate bore the remaining elements with similar amounts of gallium and germanium recovered. Less than half the amount of iron was also recovered, along with approximately 0.5  $\mu\text{g}$  of tin. The amount of tin in the gallium product solution is similar to that of the  $\text{Sn}^{4+}/\text{Ga}^{3+}$  column separation. The reason for tin being recovered in the de-ionised water eluate is still uncertain. As tin precipitates under the standard radiolabelling conditions, the gallium eluent is deemed to be of a similar purity to that of the products of the third and fourth column separations.

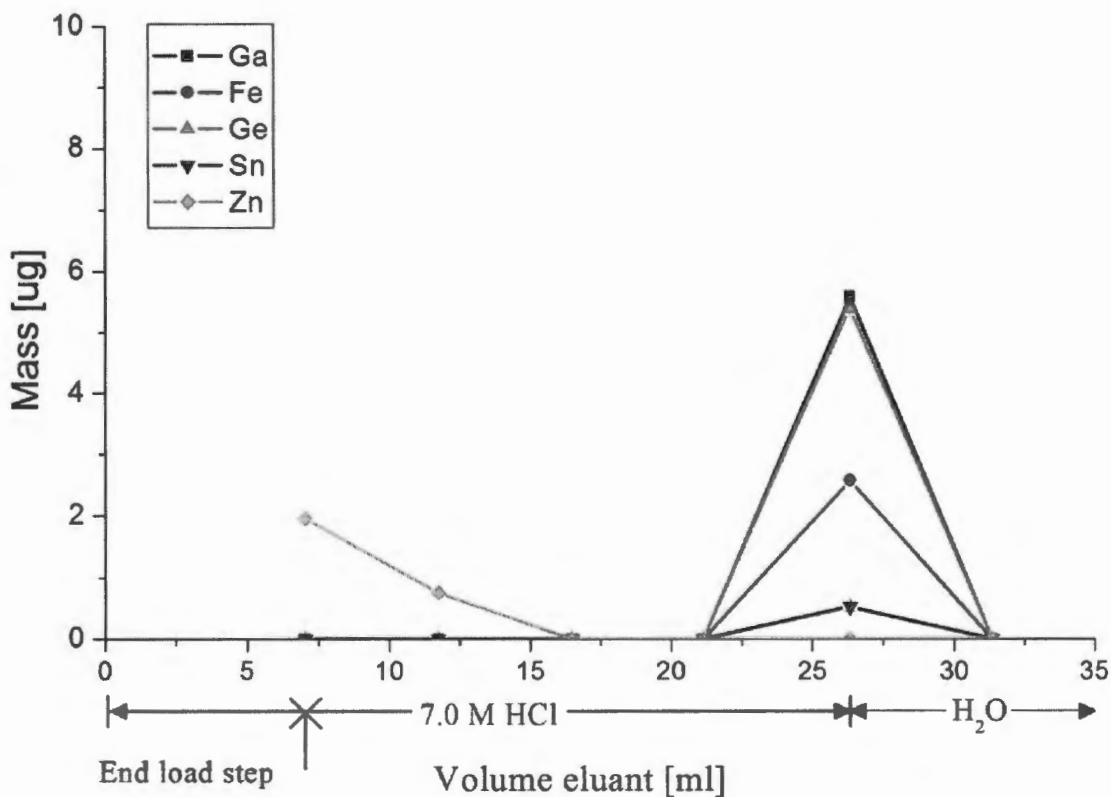


**Figure 4.11: Fifth of five column separations of ions on a 2 ml Amberchrom CG71 column**

In summary, the behaviour of each element varied between separations, although some common trends can be assumed. The bulk of the zinc was eluted in the load step and the first increment of the rinse step. Where large amounts of iron were recovered, most of it was recovered in the second and third rinse increments. During the elution of gallium, an equal amount of germanium was recovered in the first increment, with varying amounts of iron. Although the results are not directly comparable, the amount of iron recovered in the de-ionised water eluate was approximately half that of the gallium recovered, with the exclusion of the first separation. An approximate total of 1 µg of tin was recovered in two increments across all five separations.

The initial load volume cannot be adjusted, as the optimal volume of the generator eluent is 3.0 ml and requires at least 4.0 ml of concentrated HCl to correct for concentration. A minimum load volume of 7.0 ml is required for future tests. As no elements were recovered in the third rinse step, the rinse volume required was reduced from 15.0 ml to 10.0 ml to minimise the total time of separation. A rinse volume five times that of the column (i.e.  $5 \times 2$  ml) was determined as the minimum rinse volume. The elution of gallium required only 5.0 ml of the 10.0 ml used to elute the remaining elements from the column. It was determined that the volume to elute gallium should be twice that of the column volume used (i.e.  $2 \times 2$  ml). At a flow rate of 2.5 ml/min, a total volume of 22.0 ml would take approximately 9 minutes to pump through the column.

#### **4.2.4 Separation method improvements**

The separation method is required to be performed in as short a period as possible due to the short half-life of  $^{68}\text{Ga}$ . By reducing the column size used in a separation, the volumes required for rinsing and eluting the target ion can be reduced further. As the flow rate has an upper limit of 2.5-3.0 ml/min to allow for sufficient interaction of the eluent with the resin, reducing the column size is a feasible approach to minimising the total time of the separation. The same synthetic generator eluent was used as those for the individual contaminant column separations, with the addition of a 1 mCi spike of  $^{68}\text{Ga}$  supplied by a single generator elution.

This enabled the measurement of the  $^{68}\text{Ga}$  yield of the eluent by measuring the activity of the purified product, which was corrected for decay to the time of the initial load step.

Losses of activity were encountered in the separation method, therefore the effectiveness of the column size was determined by the final % yield and volume required to elute most of the activity. As any purified  $^{68}\text{Ga}$  product would need to be evaporated before radiolabelling, the elution volumes should be minimised to reduce the evaporation time. The first separation was conducted with a 2.0 ml column, as shown in Figure 4.12. Minimal losses in  $^{68}\text{Ga}$  were measured, amounting to approximately 2% of the total  $^{68}\text{Ga}$  which had been contained in the loading vial used for mixing. There was no activity lost in either the load step or the rinse step of the separation. After the column was pumped dry to remove most of the acid, 1.0 ml increments were used to elute the  $^{68}\text{Ga}$  from the column. The first and last increment yielded 5.8% of the  $^{68}\text{Ga}$ , the bulk of the activity being eluted in the second and third increment. By discarding the first and last increments of the de-ionised water eluate, 78% of the activity was recovered within a volume of 2.0 ml of de-ionised water.

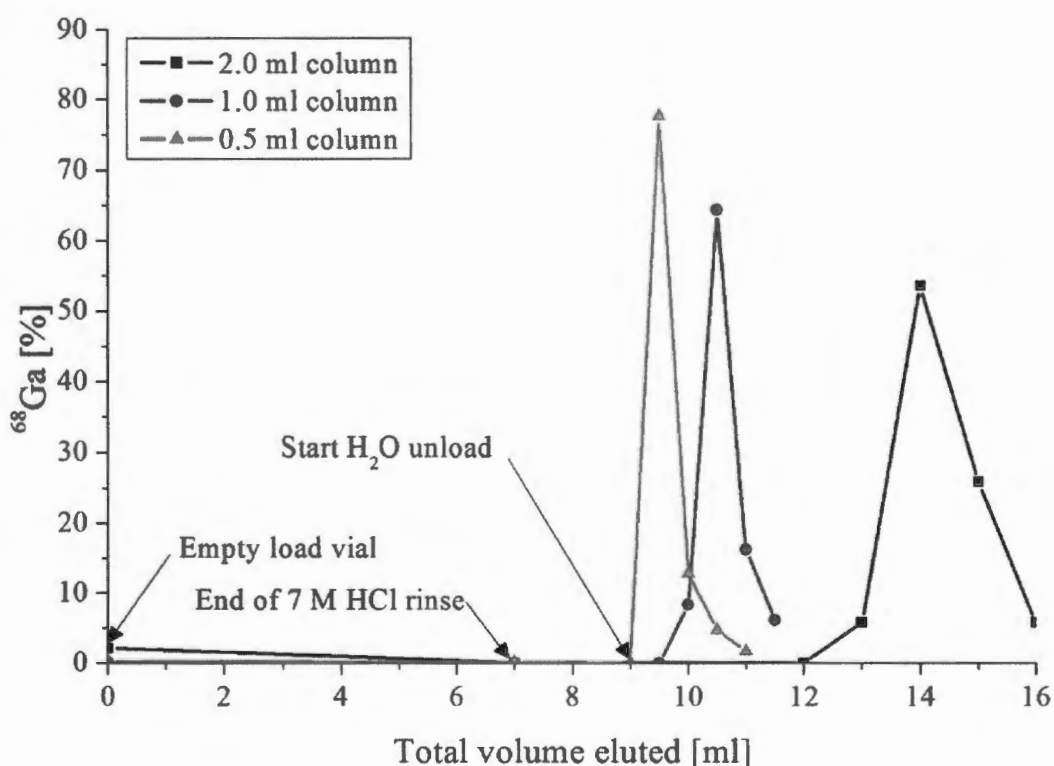


**Figure 4.12: A column separation of a  $^{68}\text{Ga}$  spike from Ge, Sn, Fe and Zn performed on 2, 1 and 0.5 ml Amberchrom CG 71 columns**

Once the 1.0 ml column had been loaded with the spiked synthetic generator eluent, the loading vial, load solution and rinse solution contained almost no activity. A similar trend was observed for both the 1.0 ml column and the 2.0 ml column, the bulk of the activity being eluted in the second and third elution volume increment. By discarding the first and last increment of the water eluate, 80% of the activity was recovered within a volume of 1.0 ml.

It can be concluded that, practically, the smallest size column for this study is 0.5 ml, because it retained all the activity on the column during the load and rinse steps. It also eluted the largest proportion of  $^{68}\text{Ga}$  during the first increment, where approximately 90% of the activity was recovered in 1.0 ml of de-ionised water eluate.

Of the three different column sizes tested, the 0.5 ml column had the highest yield, and was eluted with the first 1.0 ml of de-ionised water without the need to discard any increments. Therefore the final volumes selected for this method were: 7.0 ml for the load step, 2.5 ml for the rinse step, and 1.0 ml for the elution of  $^{68}\text{Ga}$  with de-ionised water. The time taken to pump the 10.5 ml through the column was approximately 4 minutes and 10 seconds. This reduced the original process time by approximately 3 minutes and 50 seconds.

### **4.3 Modified separation method performance**

After improving the efficiency and reducing the volume of chemicals required, the synthetic column separation method was tested on the eluent of a one year old aged  $\text{SnO}_2$   $^{68}\text{Ge}/^{68}\text{Ga}$  generator. In ion exchange chromatography, tailing is an undesirable characteristic as it shifts away from an ideal Gaussian elution peak by broadening the back end of the peak baseline. After initial tests to determine the effective yield of the separation method had been performed, excessive tailing in the elution of  $^{68}\text{Ga}$  was observed.

The gallium elution volume was then adjusted from 1.0 ml de-ionised water to 2 ml, to ensure sufficient separation from the column. The 0.5 ml column was tested at three different times in the week to account for the natural variation in generator behaviour. The same 0.5 ml column was used as described in section 4.2.3.

Losses in activity were incurred in the separation process, as reported in Table 4.2. The activities of  $^{68}\text{Ga}$  have been corrected to the time of elution respective to each separation. These losses can be attributed to the load vial, load solution, tubing and rinse solution, and account for 930  $\mu\text{Ci}$  (9.7%) of the  $^{68}\text{Ga}$  lost. The effect of tailing was made obvious by the amount of activity retained by the column despite an increase in the rinse solution to twice the volume.

**Table 4.2: Triplicate performance analysis on 0.5 ml Amberchrom CG71 column**

<b>Column separation performance</b>			
	<b>Column A</b>	<b>Column B</b>	<b>Column C</b>
<b>Initial activity [<math>\mu\text{Ci}</math>]</b>	9480	9624	9639
<b>Activity losses [<math>\mu\text{Ci}</math>]</b>			
Loading vial	120	109	204
Column	1520	1640	1274
Load and rinse solution	141	200	190
Tubing	668	40	48
<b>Yield [%]</b>	74.1	79.3	82.2
<b>Eluate [<math>\mu\text{Ci}</math>]</b>	7020	7630	7920
<b>Labelling solution [<math>\mu\text{Ci}</math>]</b>	3520	3860	3940
<b>Particle 1 [<math>\mu\text{Ci}</math>]</b>	1109	1120	1194
<b>Particle 2 [<math>\mu\text{Ci}</math>]</b>	1118	1210	1144

The column retained 1520  $\mu\text{Ci}$  (16%)  $^{68}\text{Ga}$ , leaving a final yield of 7020  $\mu\text{Ci}$  (74.1%)  $^{68}\text{Ga}$  in 2.0 ml de-ionised water. The time elapsed from the moment of measuring the initial activity to the point of elution was approximately 7 minutes and 30 seconds. The process time could be reduced further to less than 6 minutes, with practice by the operator.

With only 350  $\mu\text{Ci}$   $^{68}\text{Ga}$  (3.6%) measured, more activity was measured on the column in the second separation, with 1640  $\mu\text{Ci}$   $^{68}\text{Ga}$  (17%) retained, and fewer losses from the load vial, load solution, tubing and rinse solution.

There was a small increase in overall performance in the second separation, with 7630  $\mu\text{Ci}$   $^{68}\text{Ga}$  (79.3%) recovered in 2.0 ml de-ionised water. The separation took approximately 7 minutes to complete.

The third separation retained approximately 440  $\mu\text{Ci}$   $^{68}\text{Ga}$  (4.5%) across the separation panel and 1274  $\mu\text{Ci}$   $^{68}\text{Ga}$  (13.2%) on the column after elution. Of the three separations, the third obtained the highest total activity and yield with 7920  $\mu\text{Ci}$   $^{68}\text{Ga}$  (82.2%) in 2.0 ml of de-ionised water. The separation took approximately 8 minutes to complete.

The mean yield was calculated as  $7520 \pm 178$   $\mu\text{Ci}$   $^{68}\text{Ga}$  in 2.0 ml of the water eluate. The higher yield obtained in the enhanced separation method for the 0.5 ml column (Figure 4.12) was most likely due to the higher concentration of  $\text{Ga}^{3+}$ . As the volume of the final product was smaller than it is in the standard radiolabelling procedure, less time was required for the evaporation step. This shorter evaporation time compensates for the longer time required for the separation process and the resulting losses related to radioactive decay during evaporation. The activity recovered from each column separation was then used to test the effect of purity on the radiolabelling performance.

#### 4.4 Tracer labelling comparison test

It was not possible to use ICP spectroscopy to analyse the contaminant composition of the eluent from the  $^{68}\text{Ge}/^{68}\text{Ga}$  generator, as both  $^{68}\text{Ge}$  and  $^{68}\text{Ga}$  are radioactive and would pose a potential radiation contamination hazard to any equipment involved. As the radio-purity of  $^{68}\text{Ga}$  could not be measured directly, a radiolabelling comparison test was used to determine the effectiveness of the separation method as part of the complete radiolabelling procedure.

The standard radiolabelling procedure was performed at three different times during the week, to account for the natural variation of the  $\text{SnO}_2$   $^{68}\text{Ge}/^{68}\text{Ga}$  generator. The activity added into the equilibration vial for the standard radiolabelling procedure was higher than that of the purified  $^{68}\text{Ga}$ . The initial labelling activity referred to in Table 4.3 is the amount of  $^{68}\text{Ga}$  added to the equilibration vial at the starting time of the equilibration

process. The end labelling activity reports the amount of  $^{68}\text{Ga}$  left in the vial at the time equilibration had stopped. The relative amount of  $^{68}\text{Ga}$  activity lost to decay, without the generator eluent being purified at the end of evaporation, is less than the activity lost from the purification method at the end of evaporation (Initial labelling act., Table 4.3).

**Table 4.3: Comparison of radiolabelling performance between purified and un-purified  $^{68}\text{Ga}$  using NRW 100**

Labelling test	Column separation method			Standard radiolabelling		
	A	B	C	D	E	F
Initial labelling act. [ $\mu\text{Ci}$ ]	4787	5249	5358	5548	6661	5709
End labelling act. [ $\mu\text{Ci}$ ]	3520	3860	3940	4080	4898	4198
Particle 1 [ $\mu\text{Ci}$ ]	1109	1120	1194	1019	1025	1008
Particle 2 [ $\mu\text{Ci}$ ]	1118	1210	1144	1021	1063	960

The volume, equilibration time and particle size were kept the same for all tests in the interest of comparison for reliability. The resin beads were placed into a vial for shaking with the end labelling activity; and after 30 minutes of equilibration, the resin beads were removed. The average activity labelled on each tracer for the column separation method was  $1150 \pm 43 \mu\text{Ci } ^{68}\text{Ga}$ . The standard radiolabelling method had an average radiolabelling of  $1020 \pm 33 \mu\text{Ci } ^{68}\text{Ga}$ . Therefore, within limits of experimental uncertainty, the activity radiolabelled on the resin beads from the column separation was higher than that of the standard radiolabelling procedure, despite having a lower initial activity. An increase in  $^{68}\text{Ga}$  purity using the purification method is believed to increase the radiolabelling performance. Therefore, this method has the potential to extend the lifespan of an aged  $\text{SnO}_2 \text{ } ^{68}\text{Ge}/^{68}\text{Ga}$  generator.

The column separation method was tested again with a radiolabelling comparison test using AG50W-X4 cation exchange resin. The average activity labelled on each tracer with the column separation method was  $936 \pm 51 \mu\text{Ci } ^{68}\text{Ga}$ . The standard radiolabelling method had an average of  $932 \pm 49 \mu\text{Ci } ^{68}\text{Ga}$  (Table 4.4). For AG50W-X4, the column separation method did not improve the average radiolabelling activity. However, the method does use a lower initial labelling activity to obtain a similar labelling activity making it more efficient. Despite the lower exchange capacity of AG50W-X4 (Table 2.2),

sufficient activity (500  $\mu\text{Ci}$   $^{68}\text{Ga}$ ) was radiolabelled from a one year old  $\text{SnO}_2$   $^{68}\text{Ge}/^{68}\text{Ga}$  generator to be effectively used for PEPT studies.

**Table 4.4: Comparison of radiolabelling performance between purified and un-purified  $^{68}\text{Ga}$  using AG50W-X4**

Labelling test	Column separation method		Standard radiolabelling	
	A	B	A	B
Initial labelling act. [ $\mu\text{Ci}$ ]	4962	5110	6335	5818
End labelling act. [ $\mu\text{Ci}$ ]	3614	3725	4619	4241
Particle 1 [ $\mu\text{Ci}$ ]	878	926	893	892
Particle 2 [ $\mu\text{Ci}$ ]	942	1001	950	993

## 4.5 Summary

A literature survey suggested the presence of the contaminant ions germanium, tin, zinc and iron in the eluent of a  $^{68}\text{Ge}/^{68}\text{Ga}$   $\text{SnO}_2$  generator. In order to determine which ions would compete with  $^{68}\text{Ga}$  for uptake on an ion exchange resin in radiolabelling, distribution coefficients were determined for each contaminant ion and for two different resins NRW 100 and AG50W-X4. This indicated that  $\text{Al}^{3+}$  would be sorbed most readily by both resins. This ion can, however, be removed from the eluent by use of the purification method used in this study. Iron was shown to be a significant contaminant which in large concentrations could compete with the uptake of Ga. The cause of  $\text{Fe}^{3+}$  contamination was assumed to be environmental and was removed unsuccessfully, after which it was determined that it should be removed from all reagents and equipment prior to use. Titanium was added as a potential ion to remove iron; however its high distribution coefficient suggested that its inclusion in the separation process would increase competition with  $\text{Ga}^{3+}$  for uptake on both resins and should therefore be avoided. Zinc and germanium had lower values of  $K_d$ , suggesting that, at equal or lower concentrations, they would have interfered less so with the uptake of  $^{68}\text{Ga}$ . The precipitation of Sn under radiolabelling conditions made interference with  $\text{Ga}^{3+}$  sorption on NRW 100 and AG50W-X4 unlikely. NRW 100 had a higher selectivity than AG50W-X4 for all the ions tested.

The trends for both resins were similar, with the exception of a higher selectivity of  $Zn^{2+}$  over  $Fe^{3+}$  for NRW 100 while having the opposite for AG50W-X4.

An elution test was performed with each contaminant ion and  $Ga^{3+}$  to determine whether a column made from Amberchrom CG71 could be used to separate Ga from the other ions. The results showed that Fe and Ge could not be separated from Ga, whereas Al and Zn had been separated successfully. Any germanium in the eluent would be radioactive  $^{68}Ge$  which with a half-life of 280 days, poses a potential radioactivity contamination hazard.

Column separations were then performed for a solution containing all of the contaminant ions and  $Ga^{3+}$ , to test for any synergistic effects between ions by comparing the separations with the plotted elution profiles. Although iron was recovered in the de-ionised water eluate for all five separations, a significant amount was eluted in the rinse steps in two of the separations. Of the two increments in which tin was recovered, only 0.5  $\mu g$  was recovered in a rinse step instead of the expected gallium eluate. Germanium and zinc behaved fairly consistently across the five separations.

All separations were undertaken on the same column, to test whether the column could be used for repeat separations. Gallium and germanium both behaved consistently across all five separations. Zinc was consistently eluted in the load and rinse steps throughout almost all of the separations, the exception being a recovery of 0.5  $\mu g$  in the elution of the final product of one separation. Although iron was recovered repeatedly in the gallium elution step, some iron was recovered in the rinse step for two of the separations. Overall, the column separations yielded a fairly repeatable grade of gallium across the  $Ga^{3+}$  elutions with water and behaved consistently with recurring use.

Three different column sizes, 2.0, 1.0 and 0.5 ml, were tested to find the minimum column size required for purification. This would have the effect of reducing the solution volume and evaporation time in radiolabelling, leading to a reduction in the loss of  $^{68}Ga$  due to radioactive decay. The results showed that the 0.5 ml column was the optimum size, as there was no  $^{68}Ga$  breakthrough during the loading and rinse step, and 90% of the  $^{68}Ga$  had been recovered with the first rinsing step.

The method of purifying  $^{68}\text{Ga}$  had a significant impact on the radiolabelling efficiency, as the average radiolabelling for a 465  $\mu\text{m}$  NRW 100 resin bead was 1150  $\mu\text{Ci}$  compared with the average of 1020  $\mu\text{Ci}$  for the un-purified product. The improved radiolabelling was achieved using less activity than that for the un-purified product.

# Chapter 5

## Conclusion

Positron-emitting particle tracking is an important technique for studying engineering systems, as it provides kinematic information about the behaviour of a tracer particle that can be used to validate simulations of flow and improve fundamental physics-based models. The tracer particle must be both representative of the system under study and labelled with a positron-emitting radionuclide, such as  $^{68}\text{Ga}$ . At PEPT Cape Town, tracers are usually fabricated by ion exchange where functional groups on the surface of a resin are replaced with the target radionuclide  $^{68}\text{Ga}$ . This is supplied from a  $\text{SnO}_2$   $^{68}\text{Ge}/^{68}\text{Ga}$  generator, which is a shielded column containing a supply of the parent radionuclide  $^{68}\text{Ge}$ . The decay of  $^{68}\text{Ge}$  produces  $^{68}\text{Ga}$  as a daughter radionuclide, and the column is composed of ion exchange resins to separate  $^{68}\text{Ga}$  from the  $^{68}\text{Ge}$  supply for use in radiolabelling. However, as the generator ages, the eluent contains increasing amounts of contaminant ions such as Ge, Fe, Sn, and Zn, which originate from the decay of  $^{68}\text{Ga}$ , the breakdown of the column materials, and the surrounding environment. The contaminant ions interfere with the tracer-labelling process by competing with  $^{68}\text{Ga}$  for exchange sites on the resin. Ultimately this reduces the efficiency and consistency of the tracer-labelling process and limits the lifespan of the generator to 6 to 9 months.

This work measured the selectivity for the different contaminant ions on two resins, to predict which ions had the greatest effect on the radiolabelling process. Column separations were then performed on combinations of ions to investigate synergistic sorption effects. Based on the results of these two experiments, a purification method developed by Nadioo and van der Walt (2001) was implemented in the standard radiolabelling procedure at PEPT Cape Town. This aimed to remove the contaminants from the generator eluent and increase the sorption of  $^{68}\text{Ga}$  on an ion exchange resin.

The modified method separated zinc and aluminium successfully while reducing the amount of iron and tin recovered with gallium in the final product. Germanium was not successfully separated from gallium. An overall increase from an average labelling of 1020  $\mu\text{Ci}$  to 1150  $\mu\text{Ci}$  on the radiolabelling process was achieved using purified  $^{68}\text{Ga}$  despite a lower initial concentration of  $^{68}\text{Ga}$  than the un-purified method having been used.

Therefore the main conclusion of this work is that  $^{68}\text{Ga}$  supplied from an aged  $\text{SnO}_2$   $^{68}\text{Ge}/^{68}\text{Ga}$  generator eluent can be purified, which leads to improvement in the radiolabelling performance of the ion exchange resins NRW100 and AG50W-X4.

## 5.1 Limitations of the work

The separation method improves the performance of the radiolabelling for both strong acid cation exchange resins NRW100 and AG50W-X4. The specific physical structure of each resin makes the chemical properties of each resin unique, and thus the separation method does not apply to this work. The separation method is limited to acidic chloride media. The effect of speciation for the ions in synthetic generator eluent is assumed to be the same as that for the eluent obtained from an aged  $\text{SnO}_2$   $^{68}\text{Ge}/^{68}\text{Ga}$  generator. The naturally-occurring variations of contaminant ion concentrations are assumed to be replicated sufficiently by the experimental method to obtain consistent results. The evaporation step in the radiolabelling method has not been included in this work as it has the potential to change the speciation of the ions in the generator eluent.

## 5.2 Recommended further work

### 5.2.1 Purification of $^{68}\text{Ga}$

The equilibrium distribution coefficients for the selected elements  $\text{Ge}^{4+}$ ,  $\text{Sn}^{4+}$ ,  $\text{Ga}^{3+}$ ,  $\text{Fe}^{3+}$ ,  $\text{Al}^{3+}$ ,  $\text{Ti}^{3+}$ ,  $\text{Fe}^{2+}$  and  $\text{Zn}^{2+}$  should be determined in 7 M HCl for Amberchrom CG-71 to better understand the process and determine why the separation process did not behave as expected. The method of van der Meulen and van der Walt (2006) should be further investigated to successfully reduce  $\text{Fe}^{3+}$  in the  $^{68}\text{Ga}$  generator eluate before purification. Furthermore, the equilibrium distribution coefficients should then be determined for  $\text{Fe}^{2+}$  in 0.005 M HCl to determine whether residual  $\text{Fe}^{2+}$  will interfere with the radiolabelling process.

The purification method can be improved further to separate  $^{68}\text{Ge}$  from the eluent. Contamination of tracers and equipment with  $^{68}\text{Ge}$  poses a radiation hazard to users; therefore the complete removal of  $^{68}\text{Ge}$  from the eluent is an issue of high priority. The separation of germanium from gallium should be possible using the proposed method and should be further investigated.

The elution volume for  $^{68}\text{Ga}$  is sufficiently small to be integrated with the radiolabelling process, but a noticeable “peak tailing” limits the overall yield. Reducing the volume of de-ionised water required for eluting  $^{68}\text{Ga}$  or improving the yield would further improve the radiolabelling process. The purified  $^{68}\text{Ga}$  supply should be used with the radiolabelling method to determine if it improves the radiolabelling efficiency sufficiently for AG50W-X4 resin beads smaller than 100  $\mu\text{m}$  in diameter.

### 5.2.2 System enhancements

The standard radiolabelling procedure makes use of an evaporation step to adjust the pH of the  $^{68}\text{Ga}$  product. The process requires evaporating approximately 3 ml of the generator eluent over a duration of 25 to 35 minutes. The scope of this thesis has been limited to the purification method, although a prototype heating system has been developed. To reduce

the evaporation time, a vacuum system comprising a chemically resistant diaphragm pump and gas scrubber was integrated into a custom-built aluminium heating block. The initial results report an increased evaporation time of approximately 10 minutes longer than that of the current heating system. By further modifying the heating system and adjusting the airflow of the vacuum system, it is assumed that the proposed system can be improved to achieve a shorter evaporation time than that for the current system. The high temperatures required to improve the evaporation time should be reduced, since losses are incurred in the evaporation step due to a fraction of the  $^{68}\text{Ga}$  becoming insoluble when overheated.

## References

- Anderson, B.G., van Santen, R.A., de Jong, A.M., 1999. Positrons as in situ probes of transient phenomena. *Topics in Catalysis*. **8**, 125–131.
- Badawy, N.A., El-Bayaa, A.A., Abdel-Aal, A.Y., Garamon, S.E., 2009. Chromatographic separations and recovery of lead ions from a synthetic binary mixtures of some heavy metal using cation exchange resin. *Journal of Hazardous Materials*. **166**, 1266–71.
- Bbosa, L.S., Govender, I., Mainza, A. N., Powell, M.S., 2011. Power draw estimations in experimental tumbling mills using PEPT. *Minerals Engineering*. **24**, 319–324.
- Buffler, A., Govender, I., Cilliers, J. J., Parker, D. J., Franzidis, J-P., Mainza, A. N., Newman, R. T., Powell, M., van der Westhuizen, A. (2010). PEPT Cape Town : a new positron emission particle tracking facility at iThemba LABS. In *Proceedings of International Topical Meeting on Nuclear Research Applications and Utilization of Accelerators* (pp. 1–8).
- Chan, C.W., Seville, J., Fan, X., Baeyens, J., 2009. Solid particle motion in a standpipe as observed by Positron Emission Particle Tracking. *Powder Technology*. **194**, 58–66.
- Chan, C.W., Seville, J., Yang, Z., Baeyens, J., 2009. Particle motion in the CFB riser with special emphasis on PEPT-imaging of the bottom section. *Powder Technology*. **196**, 318–325.
- Cole, K., Buffler, A., Cilliers, J.J., Govender, I., Heng, J.Y.Y., Liu, C., Parker, D.J., Shah, U.V., van Heerden, M., Fan, X., 2014. A surface coating method to modify tracers for positron emission particle tracking (PEPT) measurements of froth flotation. *Powder Technology*. **263**, 26–30.
- Cole, K.E., Buffler, A., van der Meulen, N.P., Cilliers, J.J., Franzidis, J-P., Govender, I., Liu, C., van Heerden, M.R., 2012. Positron emission particle tracking measurements with 50 micron tracers. *Chemical Engineering Science*. **75**, 235–242.

- Cole, K., Hadler, K., Cilliers, J.J., 2013. Developments in positron emission particle tracking measurements of froth flotation., in: *proceedings of the Flotation 2013, MEI Flotation Conference*.
- Cole, K., Waters, K., Fan, X., 2010. Combining Positron Emission Particle Tracking and image analysis to interpret particle motion in froths. *Minerals Engineering*. **23**, 1036–1044.
- De Blois, E., Sze Chan, H., Naidoo, C., Prince, D., Krenning, E.P., Breeman, W.A.P., 2011. Characteristics of SnO<sub>2</sub>-based <sup>68</sup>Ge/<sup>68</sup>Ga generator and aspects of radiolabelling DOTA-peptides. *Applied Radiation and Isotopes*. **69**, 308–15.
- Depypere, F., Pieters, J.G., Dewettinck, K., 2009. PEPT visualisation of particle motion in a tapered fluidised bed coater. *Journal of Food Engineering*. **93**, 324–336.
- Fan, X., Parker, D.J., and Smith, M.D. (2006a). Labelling a single particle for positron emission particle tracking using direct activation and ion-exchange techniques. *Nuclear Instruments and Methods A*. **562**(1), 345–350.
- Fan, X., Parker, D.J., and Smith, M.D. (2006b). Enhancing <sup>18</sup>F uptake in a single particle for positron emission particle tracking through modification of solid surface chemistry. *Nuclear Instruments and Methods A*. **558**(2), 542–546.
- Greenwood, N.N. and Earnshaw, A. (Second E. (Eds.). (2006). *Chemistry of the Elements*. Oxford: Butterworth-Heinemann. (pp. 216–267).
- Griffiths, W.D., Beshay, Y., Parker, D.J., Fan, X., 2008. The determination of inclusion movement in steel castings by positron emission particle tracking (PEPT). *Journal of Material Science*. **43**, 6853–6856.
- Griffiths, W.D., Beshay, Y., Caden, A. J., Fan, X., Gargiuli, J., Leadbeater, T.W., Parker, D.J., 2011. The Use of Positron Emission Particle Tracking (PEPT) to Study the Movement of Inclusions in Low-Melting-Point Alloy Castings. *Metallurgical and Material Transactions B*. **43**, 370–378.
- Hawkesworth, M.R., O'Dwyer, M.A., Walker, J., Fowles, P., Heritage, J., Stewart, P.A.E., Witcomb, R.C., Bateman, J.E., Connolly, J.F., Stephenson, R., 1986. A positron camera for industrial application. *Nuclear Instruments and Methods A*. **253**, 145–157.
- Kunin, R., 1951. Ion Exchange. *Analytical Chemistry*. **23**, 45–46.
- Kuo, H.P., Knight, P.C., Parker, D.J., Burbidge, A. S., Adams, M.J., Seville, J.P.K., 2003. Non-equilibrium particle motion in the vicinity of a single blade. *Powder Technology*. **132**, 1–9.
- Laurent, B.F.C., Bridgwater, J., Parker, D.J., 2002. Convection and segregation in a horizontal mixer. *Powder Technology*. **123**, 9–18.

- Levin, C., Hoffman, E., 1999. Calculation of positron range and its effect on the fundamental limit of positron emission tomography system spatial resolution. *Physics in medicine and Biology*. **44**, 781-799.
- Loc'h, C., Mazière, B., Comar, D., 1980. A New Generator for Ionic Gallium-68. *The Journal of Nuclear Medicine*. **21**, 171-173.
- McElvany, K.D., Hopkins, K.T., Welch, M.J., 1984. Comparison of  $^{68}\text{Ge}/^{68}\text{Ga}$  generator systems for radiopharmaceutical production. *The International Journal of Applied Radiation and Isotopes*. **35**, 521-524.
- Moses, W.W., 2011. Fundamental limits of spatial resolution in PET. *Nuclear Instruments and Methods A*. **648**, 236-240.
- Naidoo C., 1998. *The production of gallium-67 by proton induced nuclear reactions on a tandem  $^{nat}\text{Ge}/^{nat}\text{Zn}$  target*. University of Cape Town, South Africa. MSc.
- Naidoo, C., van der Walt, T.N., 2001. Cyclotron production of  $^{67}\text{Ga}(\text{III})$  with a tandem  $^{nat}\text{Ge}-^{nat}\text{Zn}$  target. *Applied Radiation and Isotopes*. **54**, 915-9.
- Naidoo, C., van der Walt, T.N., Raubenheimer, H.G., 2002. Cyclotron production of  $^{68}\text{Ge}$  with a  $\text{Ga}_2\text{O}$  target. *Journal of Radioanalytical and Nuclear Chemistry*. **253**, 221-225.
- Parker, D.J., Broadbent, C.J., Fowles, P., Hawkesworth, M.R., McNeil, P., 1993. Positron emission particle tracking - a technique for studying flow within engineering equipment. *Nuclear Instruments and Methods A*. **326**, 592-607.
- Parker, D.J., Fan, X., 2008. Positron emission particle tracking—Application and labelling techniques. *Particuology*. **6**, 16-23.
- Parker, D.J., Dijkstra, A. E., Martin, T.W., Seville, J.P.K., 1997. Positron emission particle tracking studies of spherical particle motion in rotating drums. *Chemical Engineering Science*. **52**, 2011-2022.
- Phelps, M.E., Hoffman, E.J., Huang, S.C., Ter-Pogossian, M.M., 1975. Effect of positron range on spatial resolution. *Journal of Nuclear Medicine*. **16**, 649-652.
- Sen, K., Breeman, W.A.P., Wolterbeek, H.T., 2011. Choice of Inorganic Materials as  $^{68}\text{Ge}/^{68}\text{Ga}$  Generator : An Intercomparison. *Ion Exchange Letters*. **4**, 32-43.
- Smith-Jones, P.M., Strelow, F.W.E., Böhmer, R.G., 1986. The separation of carrier-free  $^{85}\text{Sr}$  from a rubidium chloride cyclotron target. *International Journal of Radiation and Applied Isotopes*. **37**, 240-242.
- Spinks, T., Jones, T., Bloomfield, P.M., Bailey, D.L., Miller, M., Hogg, D., Jones, W.F., Vaigneur, K., Reed, J., Young, J., 2000. Physical characteristics of the ECAT EXACT3D positron tomograph. *Physics in Medicine and Biology*. **45**, 2601.

- Stellema, C.S., Vlek, J., Mudde, R.F., de Goeij, J.J.M., van den Bleek, C.M., 1998. Development of an improved positron emission particle tracking system. *Nuclear Instruments and Methods A*. **404**, 334–348.
- Strelow, F.W.E., 1980. Quantitative separation of gallium from zinc, copper, indium, iron(III) and other elements by cation-exchange chromatography in hydrobromic acid—acetone medium. *Talanta*. **27**, 231–236.
- Strelow, F.W.E. 1984. Distribution coefficients and cation-exchange behaviour of 45 elements with a macroporous resin in hydrochloric acid/methanol mixtures. *Analytica Chimica Acta*. **160**, 31–45.
- Strelow, F.W.E., 1988. Distribution coefficients and ion-exchange selectivities for 46 elements with a macroporous cation-exchange resin in hydrochloric acid-acetone medium. *Talanta*. **35**, 385–395.
- Strelow, F.W.E., Rethemeyer, R., Bothma, C.J.C., 1965. Ion Exchange Selectivity Scales for Cations in Nitric Acid and Sulfuric Acid Media with a Sulfonated Polystyrene Resin. *Analytical Chemistry*. **37**, 106–111.
- Strelow, F.W.E., Sondorp, H., 1972. Distribution coefficients and cation-exchange selectives of elements with AG50W-X8 resins in perchloric acid. *Talanta*. **19**, 1113–1120.
- Strelow, F.W.E., van der Walt, T.N., 1987. Separation of trace amounts of indium, gallium and aluminium from each other by cation-exchange chromatography on AG50-X4 resin. *Talanta*. **34**, 895–897.
- Strelow, F.W.E., Victor, A.H., Van Zyl, C.R., Eloff, C., 1971. Distribution coefficients and cation exchange behavior of elements in hydrochloric acid-acetone. *Analytical Chemistry*. **43**, 870–876.
- Van der Meulen, N.P., 2008. *The cyclon production of selected radionuclides using medium energy protons*. University of Stellenbosch, South Africa. PhD.
- Van der Meulen, N. P., van der Walt, T.N., 2007. The separation of Fe from Ga to produce ultrapure  $^{67}\text{Ga}$ . *Zeitschrift fuer Naturforschung B: Chemical Sciences*. **62**, 483–486.
- Van de Velden, M., Baeyens, J., Seville, J.P.K., Fan, X., 2008. The solids flow in the riser of a Circulating Fluidised Bed (CFB) viewed by Positron Emission Particle Tracking (PEPT). *Powder Technology*. **183**, 290–296.
- Van der Westhuizen, A. P., Govender, I., Mainza, A. N., Rubenstein, J., 2011. Tracking the motion of media particles inside an IsaMill<sup>TM</sup> using PEPT. *Minerals Engineering*. **24**, 195–204.
- Van Heerden, M.R., 2010. *The purification of  $^{68}\text{Ga}$  from an aged  $^{68}\text{Ge}/^{68}\text{Ga}$  generator and the labelling of the product and  $^{18}\text{F}$  in ion exchange for PEPT studies*. Cape Peninsula University of Technology, South Africa, BTech.

- Van Heerden M.R., 2012. *The performance analysis of AG MP-1 anion exchange resin  $^{68}\text{Ge}/^{68}\text{Ga}$  generators and the radiolabelling of ion exchange resins for PEPT studies*. Cape Peninsula University of Technology, South Africa. MTech.
- Waters, K.E., Rowson, N. A., Fan, X., Parker, D.J., Cilliers, J.J., 2008. Positron emission particle tracking as a method to map the movement of particles in the pulp and froth phases. *Minerals Engineering*. **21**, 877–882.
- Wildman, R.D., Parker, D.J., 2002. Coexistence of Two Granular Temperatures in Binary Vibrofluidized Beds. *Physical Review Letters*. **88**.
- Zagorodini, A.A., 2006. *Ion Exchange Materials-Properties and Applications*. Elsevier, Amsterdam, The Netherlands.
- Zhernosekov, K.P., Filosofov, D. V, Baum, R.P., Aschoff, P., Bihl, H., Razbash, A. A, Jahn, M., Jennewein, M., Rösch, F., 2007. Processing of generator-produced  $^{68}\text{Ga}$  for medical application. *Journal of Nuclear Medicine*. **48**, 1741–1748.
- AMBERCHROM<sup>®</sup> CG71, *Chromatographic Grade Resin*. Product data sheet.
- BioRad. (n.d.). AG 50W and AG MP-50 Cation Exchange Resins-Instruction Manual.
- IAEA, 2006. Directory of Cyclotrons used for Radionuclide Production in Member States.
- iThemba Laboratory for Accelerator-Based Sciences, Radionuclides- Background, 2013. Available from: [http://tlabs.ac.za/?page\\_id=282](http://tlabs.ac.za/?page_id=282). [25 June 2014].
- Shaner, K. (2010). *Material safety data sheet NRW100* (pp. 1–8).